

NASA  
TP  
1352  
c.1

NASA Technical Paper 1352

LOAN COPY: RETURN  
A1 WL TECHNICAL LIBR  
KIRTLAND AFB, N. M

TECH LIBRARY KAFB, NM  
01343869

# Stability and Control Characteristics of a Monoplanar Elliptic Missile Model at Mach Numbers From 1.60 to 2.86

Wallace C. Sawyer and Giuliana Sangiorgio

FEBRUARY 1979





NASA Technical Paper 1352

Stability and Control Characteristics  
of a Monoplanar Elliptic Missile Model  
at Mach Numbers From 1.60 to 2.86

Wallace C. Sawyer and Giuliana Sangiorgio  
*Langley Research Center*  
*Hampton, Virginia*

**NASA**

National Aeronautics  
and Space Administration

**Scientific and Technical  
Information Office**

1979

## SUMMARY

An investigation has been conducted of a monoplanar maneuverable missile concept having a nose forebody with a circular cross section and a centerbody and afterbody with elliptical cross sections. The tests involved several component changes and were conducted in the low Mach number test section of the Langley Unitary Plan wind tunnel at Mach numbers of 1.60, 2.16, and 2.86, at angles of attack ranging from  $-4^{\circ}$  to  $28^{\circ}$ , and at sideslip angles ranging from  $-4^{\circ}$  to  $8^{\circ}$ .

The most significant result was that at the highest Mach number (2.86), the configuration with the infrared nose produced nearly twice the axial force as the same configuration with the radar nose. The cranked wing had a destabilizing effect on the longitudinal stability and had no effect on the lateral-directional stability. The nose strakes had no effect longitudinally and were detrimental to the lateral-directional stability.

## INTRODUCTION

A continuing research program has been under way at the National Aeronautics and Space Administration for several years to provide a broader technological base for monoplanar maneuverable missile concepts. (See refs. 1 to 3.) The monoplanar concept is aerodynamically interesting because it provides a natural shape for conformational carriage. In addition, the concept provides generally higher range efficiency and, if maneuvered with pitch-roll control logic, offers good terminal maneuver capability (ref. 1).

As part of this technological effort, a limited number of configuration variables have been tested for a maneuverable air-to-air missile configuration concept (MAAM) currently under study (ref. 2). Tests were conducted at Mach numbers of 1.60, 2.16, and 2.86, with angles of attack ranging from  $-4^{\circ}$  to  $28^{\circ}$ , and sideslip angles ranging from  $-4^{\circ}$  to  $8^{\circ}$ . The limited testing considered minor configuration variables which included cranked wing, nose strakes, and nose shape.

## SYMBOLS

The coefficients of force and moment are referred to the body-axis system with aerodynamic moments about a point 40.335 cm aft of the radar nose configuration. This point of reference was used in order to correspond to the data of reference 2. The physical quantities are given in the International System of Units (SI). (See ref. 4.)

$C_A$	axial-force coefficient, $\frac{\text{Axial force}}{qS}$
$C_{A,b}$	base axial-force coefficient
$C_l$	rolling-moment coefficient, $\frac{\text{Rolling moment}}{qSd}$
$C_{l\beta}$	$= \frac{\Delta C_l}{\Delta \beta}$ , per deg
$C_m$	pitching-moment coefficient, $\frac{\text{Pitching moment}}{qSd}$
$C_N$	normal-force coefficient, $\frac{\text{Normal force}}{qS}$
$C_n$	yawing-moment coefficient, $\frac{\text{Yawing moment}}{qSd}$
$C_{n\beta}$	$= \frac{\Delta C_n}{\Delta \beta}$ , per deg
$C_Y$	side-force coefficient, $\frac{\text{Side force}}{qS}$
$C_{Y\beta}$	$= \frac{\Delta C_Y}{\Delta \beta}$ , per deg
$d$	model reference diameter, 0.0582 m
$M$	free-stream Mach number
$q$	free-stream dynamic pressure, Pa
$S$	model reference area, 0.00265 m <sup>2</sup>

$\alpha$	model angle of attack, deg
$\beta$	model angle of sideslip, deg
$\delta_p$	pitch control deflection angle (positive deflection gives positive pitching moment), deg
$\delta_r$	yaw control deflection angle (positive deflection gives positive yawing moment), deg
$\delta_a$	roll control deflection angle (positive deflection gives positive rolling moment), deg

Component designations:

B	body
T <sub>1</sub>	tail
W <sub>C</sub>	wing with cranked leading edge
W	wing with 45° swept leading edge
N <sub>S</sub>	nose strakes
I <sub>N</sub>	infrared nose
R <sub>N</sub>	radar dome nose

MODEL

Details and dimensions of the elliptical model components are shown in figure 1. The model that was tested represented a maneuverable monoplanar missile having an elliptic cross section throughout the afterbody and centerbody, a circular cross-section nose, and four tail control fins. The configurations tested involved five different combinations of the following components: cranked wing, nose strakes, radar nose, infrared nose, and a set of tail fins. The four tail fins were used to provide pitch, yaw, and roll control.

WIND TUNNEL

The investigation was conducted in the low Mach number test section of the Langley Unitary Plan wind tunnel, which is a variable-pressure, continuous-flow facility. The test section is approximately 2.13 m long and 1.22 m square. The nozzle leading to the test section has an asymmetric sliding block which permits a continuous variation in Mach number from about 1.5 to 2.9.

## TEST CONDITIONS

Tests were performed at the following tunnel conditions:

Mach number	Stagnation temperature, K	Stagnation pressure, kPa	Reynolds number per meter
1.60	311	54.6	$6.6 \times 10^6$
2.16	311	68.5	6.6
2.86	311	98.4	6.6

The dew point was maintained low enough to insure negligible condensation effects. All tests were performed with boundary-layer transition strips on the body 3.05 cm aft of the nose and 1.02 cm aft of the leading edges measured streamwise on both sides of the wing and tail surfaces. The transition strips were approximately 0.16 cm wide and were composed of No. 50 sand grains sprinkled in acrylic plastic.

## MEASUREMENTS

Aerodynamic forces and moments on the model were measured by means of a six-component electrical strain-gage balance which was housed within the model. The balance was attached to a sting which, in turn, was rigidly fastened to the tunnel support system. Balance-chamber pressure and base pressure were measured by means of static-pressure orifices located in the vicinity of the balance. Axial force was corrected for conditions of free-stream static pressure acting over the entire base of the model.

## PRESENTATION OF RESULTS

	Figure
Longitudinal aerodynamic characteristics for body-tail <sub>1</sub> , cranked wing, nose strakes, and radar nose configuration with pitch control . . . . .	2
Longitudinal aerodynamic characteristics for body-tail <sub>1</sub> , cranked wing, nose strakes, and radar nose configuration with roll control . . . . .	3
Longitudinal aerodynamic characteristics for body-tail <sub>1</sub> , cranked wing, nose strakes, and radar nose configuration with yaw control . . . . .	4
Effect of wing planform shape on longitudinal aerodynamic characteristics for body-tail <sub>1</sub> , nose strakes, and radar nose configuration . . . . .	5
Effect of nose strakes on longitudinal aerodynamic characteristics for body-tail <sub>1</sub> , cranked wing, and radar nose configuration . . . . .	6

Effect of nose shape on longitudinal aerodynamic characteristics for body-tail <sub>1</sub> , cranked wing, and nose strakes configuration . . . . .	7
Effect of nose strakes on lateral-directional characteristics for straight wing configuration . . . . .	8
Effect of nose strakes on lateral-directional characteristics for cranked wing configuration . . . . .	9
Directional stability characteristics for body-tail <sub>1</sub> , cranked wing, nose strakes, and radar nose configuration in sideslip at angle of attack . . . . .	10
Roll control characteristics for body-tail <sub>1</sub> , cranked wing, nose strakes, and radar nose configuration . . . . .	11
Yaw control characteristics for body-tail <sub>1</sub> , cranked wing, nose strakes, and radar nose configuration . . . . .	12
Variation of base drag at angle of attack for body-tail <sub>1</sub> , cranked wing, nose strakes, and radar nose configuration . . . . .	13

## RESULTS AND DISCUSSION

The comparison of the longitudinal aerodynamic characteristics for the configuration concepts tested is shown in figures 2 to 7. In general, all configurations exhibited a slight pitch-down tendency with increased angle of attack. The addition of the strake to the basic wing resulted in a slight decrease in stability at 0° angle of attack and a slight increase in linearity of the pitch curves. As expected, the bluntness of the infrared nose produced nearly twice the axial force produced by the radar nose.

The basic lateral-directional stability data are presented in figures 8 and 9 for the nose strakes ( $N_G$ ) and cranked wing ( $W_C$ ). These derivatives were taken from sideslip angles ranging from 0° to 3°. The fundamental linearity of the lateral-directional stability derivatives is demonstrated in figure 10. All the configuration concepts show a high loss of directional stability with increased angle of attack, especially at the lower Mach numbers. The addition of the strakes to the basic wing configuration had no effect on the lateral-directional stability. However, addition of the nose strakes proved to be detrimental to lateral-directional stability characteristics.

The lateral-directional control data in figures 11 and 12 indicate that sufficient control is available to overcome the directional instability for the configurations investigated in this study.

## CONCLUDING REMARKS

Wind-tunnel tests were conducted in the low Mach number test section of the Langley Unitary Plan wind tunnel in order to extend the data base for a specific monoplanar missile concept and to investigate the aerodynamic effects of minor configuration variables.

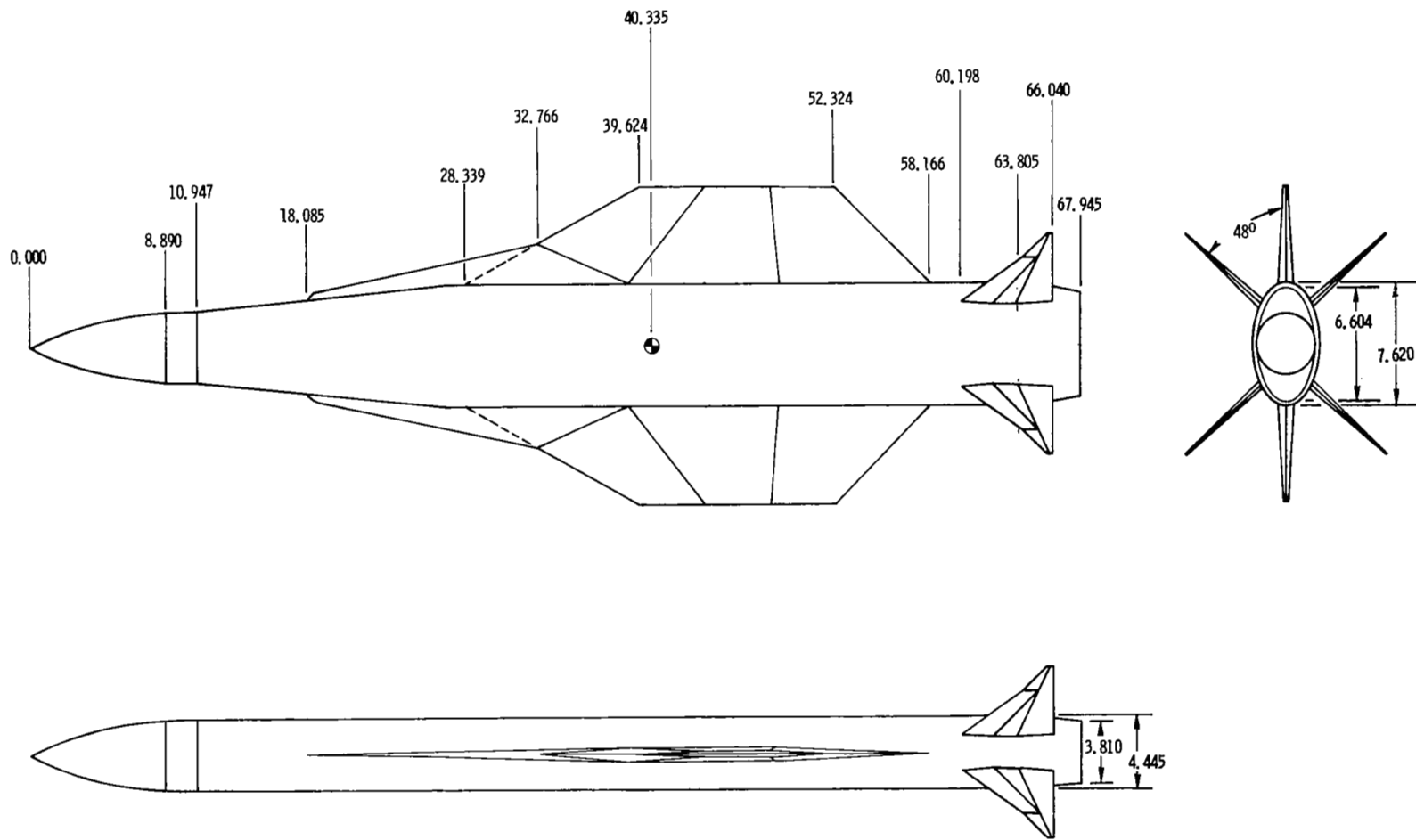
The most significant result was that at the highest Mach number (2.86), the configuration with the infrared nose produced nearly twice the axial force produced by the radar nose. The cranked wing had a destabilizing effect on the longitudinal stability and had no effect on the lateral-directional stability. The nose strakes had no effect longitudinally and were detrimental to the lateral-directional stability.

Langley Research Center  
National Aeronautics and Space Administration  
Hampton, VA 23665  
January 19, 1979

## REFERENCES

1. Sawyer, Wallace C.; Jackson, Charlie M., Jr.; and Blair, A. B., Jr.: Aerodynamic Technologies for the Next Generation of Missiles. Paper presented at the AIAA/ADPA Tactical Missile Conference (Gaithersburg, Maryland), Apr. 27-28, 1977.
2. Smith, Dale K.: Aerodynamic Characteristics of Three Maneuvering Air-to-Air Missile Models at Mach Numbers From 0.5 to 1.6. AEDC-TR-77-25, AFATL-TR-77-3, U.S. Air Force, June 1977. (Available from DDC as AD B018 815L.)
3. Graves, Ernard B.: Aerodynamic Characteristics of a Monoplanar Missile Concept With Bodies of Circular and Elliptical Cross Sections. NASA TM-74079, 1977.
4. Mechtly, E. A.: The International System of Units - Physical Constants and Conversion Factors (Second Revision). NASA SP-7012, 1973.





(a) BWCRNT1.

Figure 1.- Details of model configurations. Model dimensions are in centimeters unless otherwise noted.

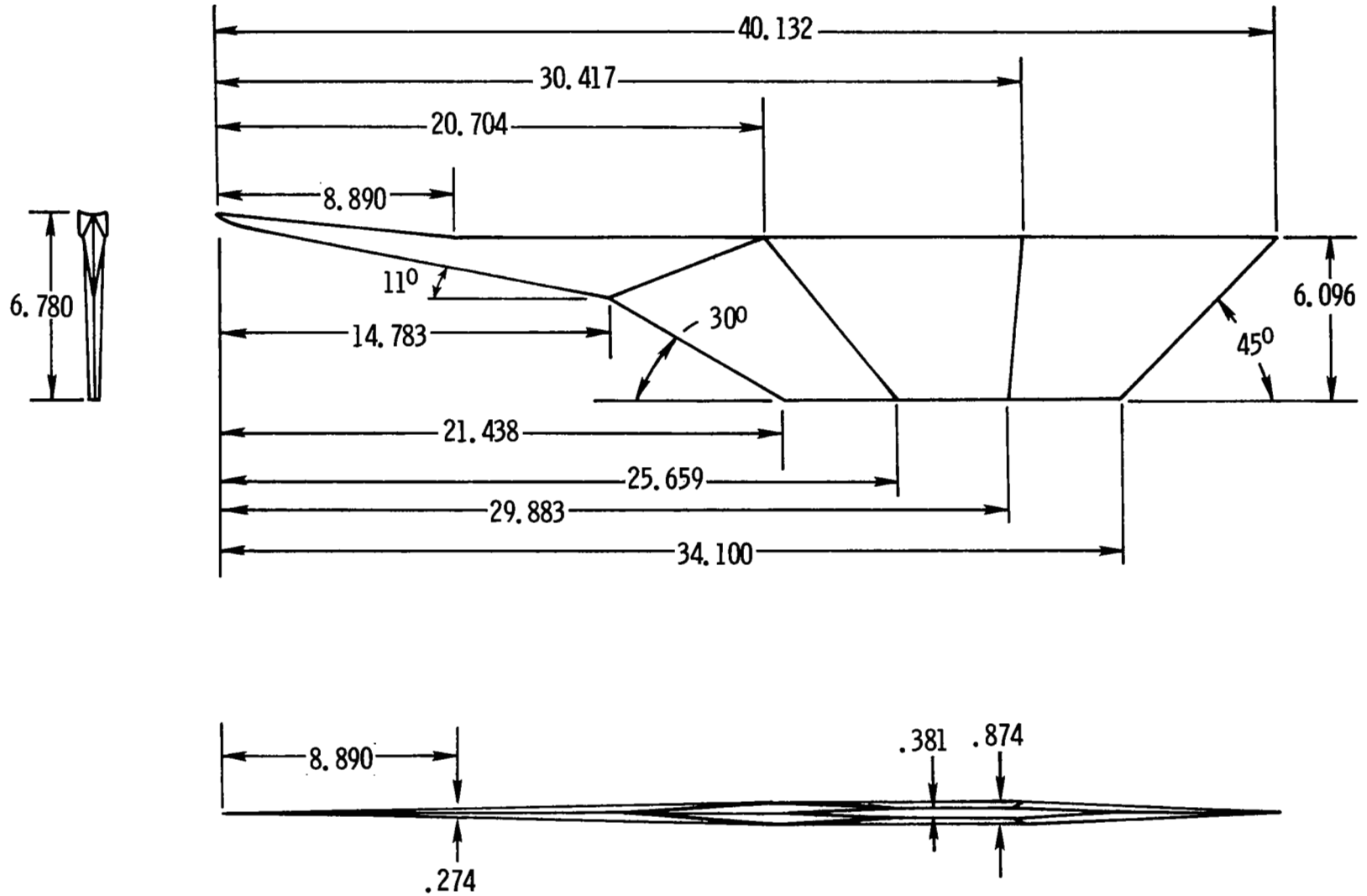
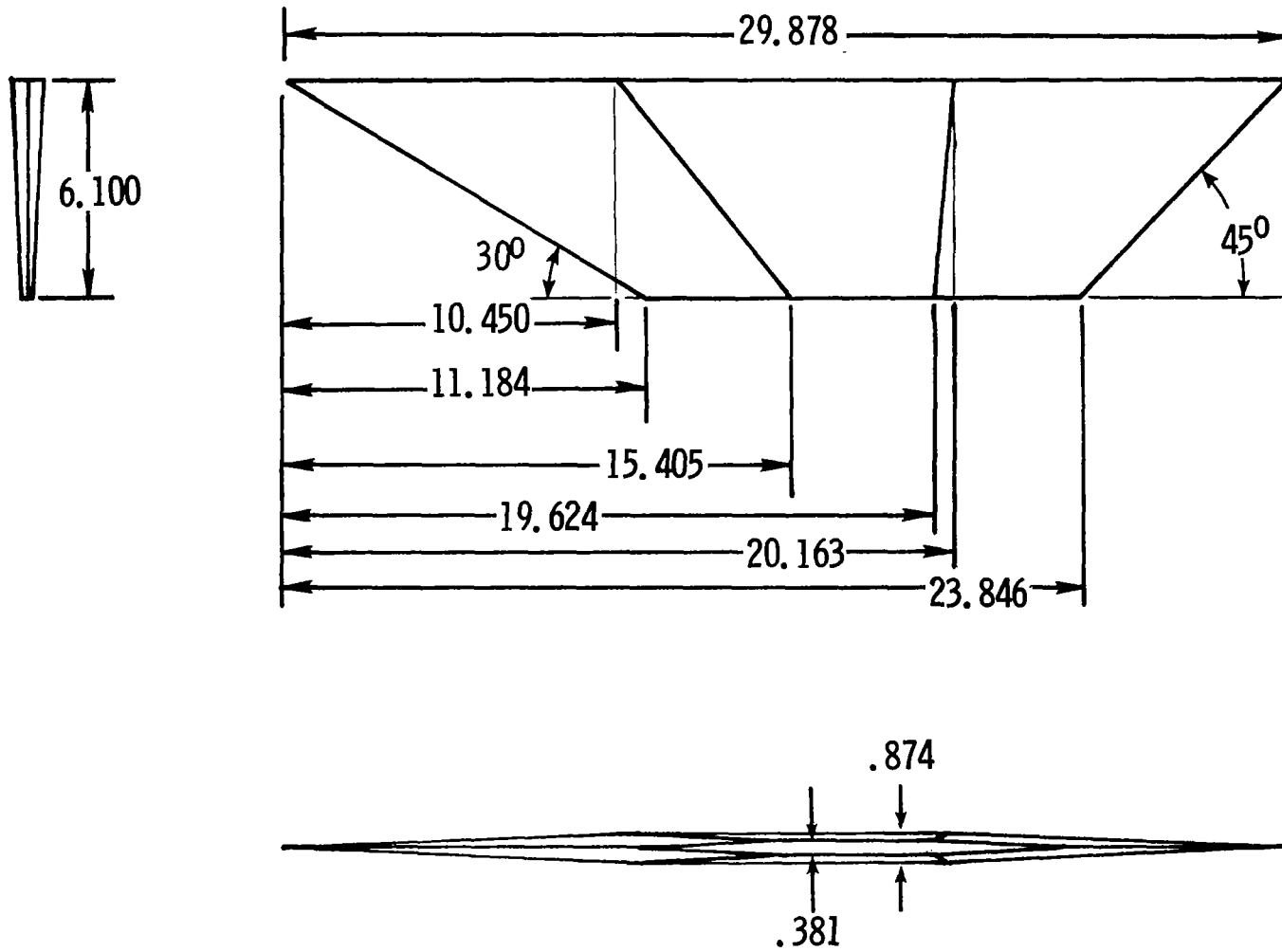
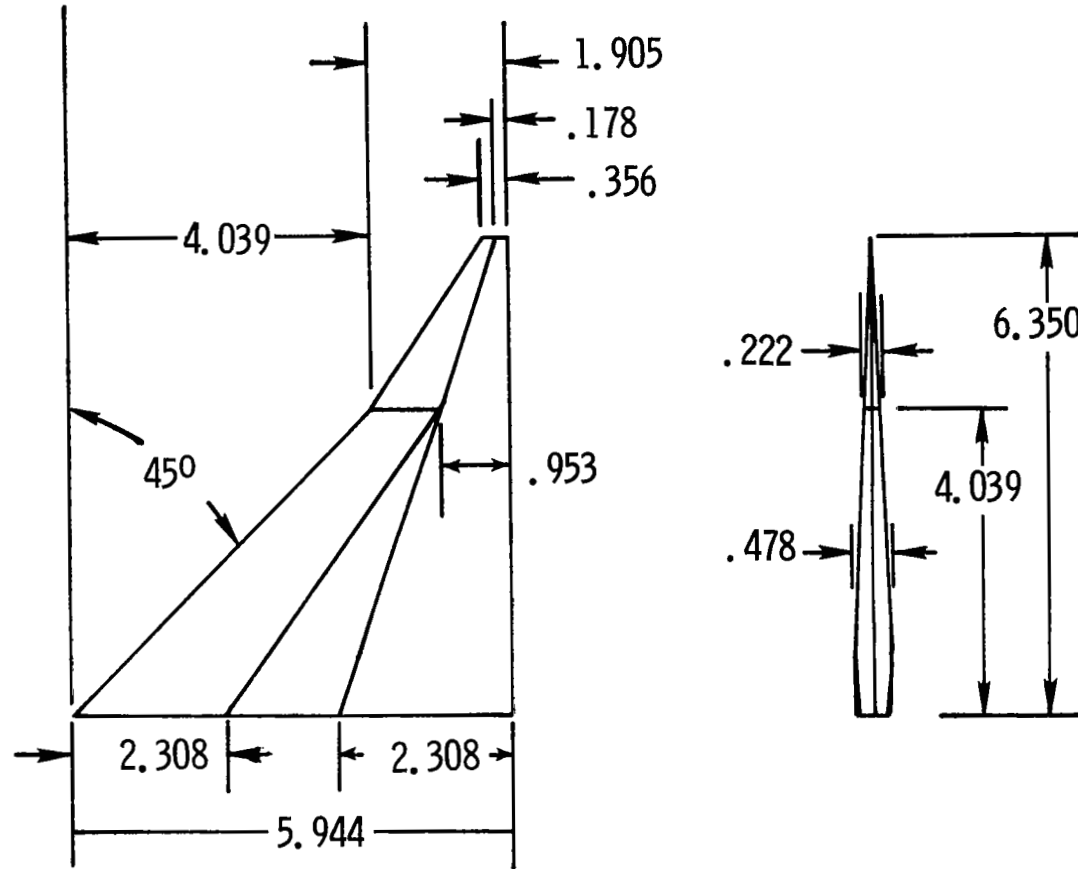
(b) Cranked wing,  $W_C$ .

Figure 1.- Continued.



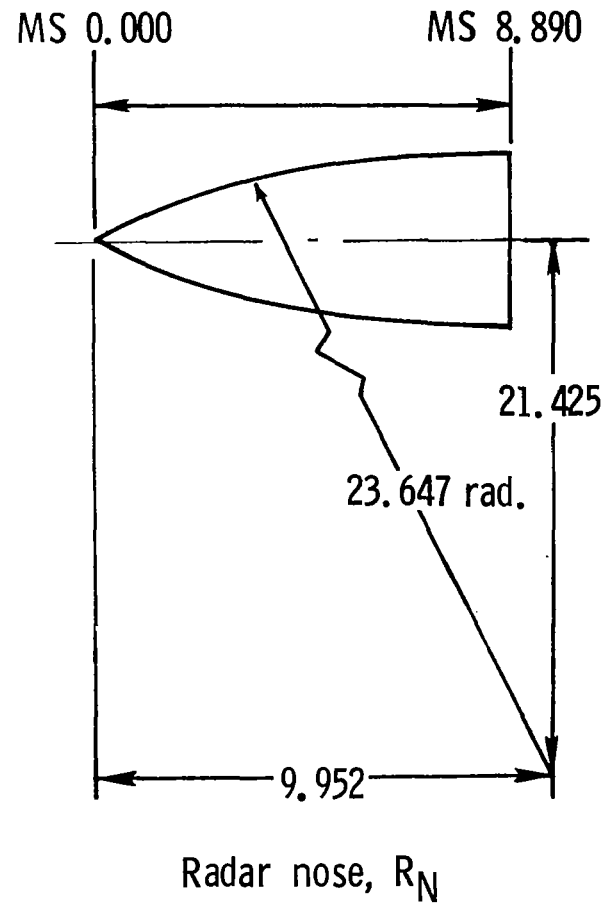
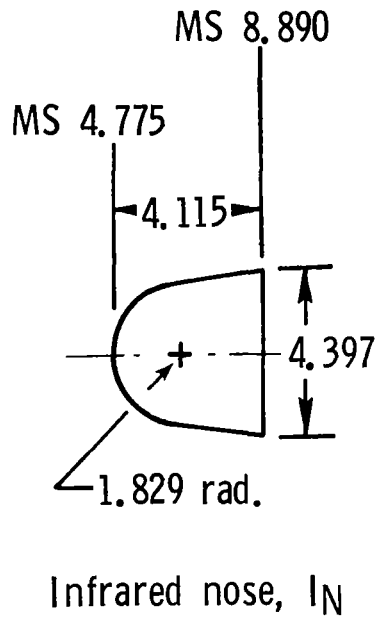
(c) Wing, W.

Figure 1.- Continued.



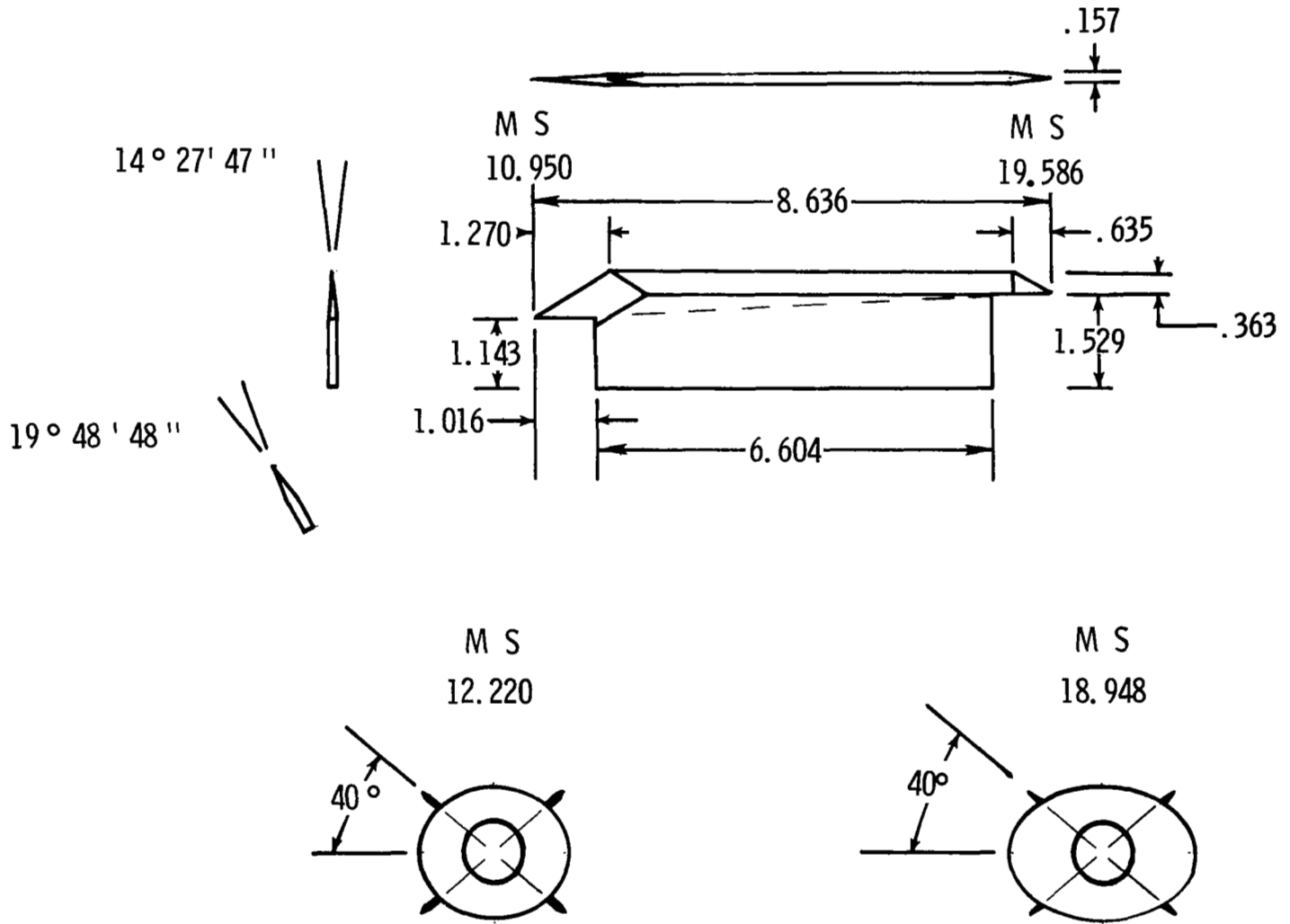
(d) Tail, T<sub>1</sub>.

Figure 1.- Continued.



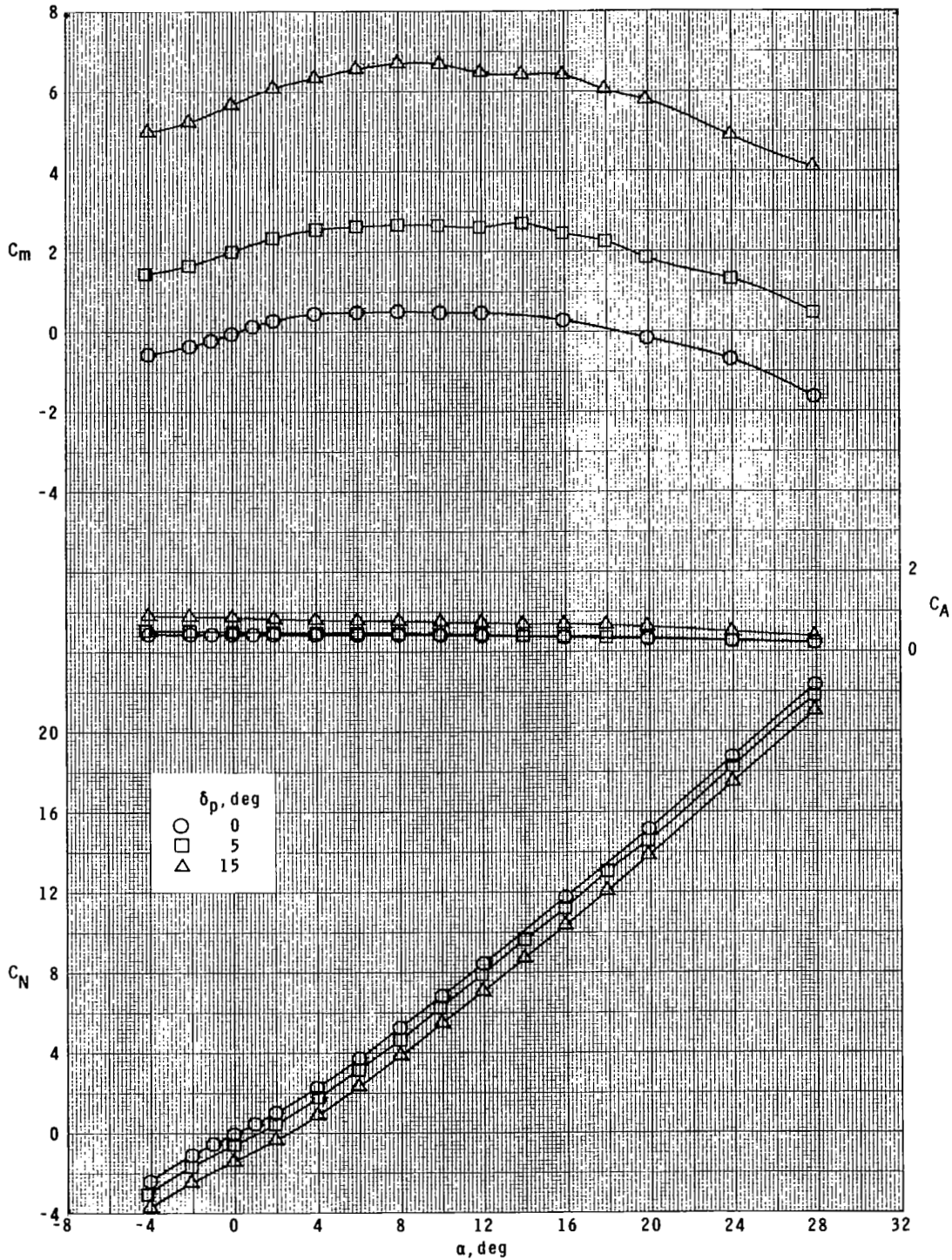
(e) Noses used on model configurations.

Figure 1.- Continued.



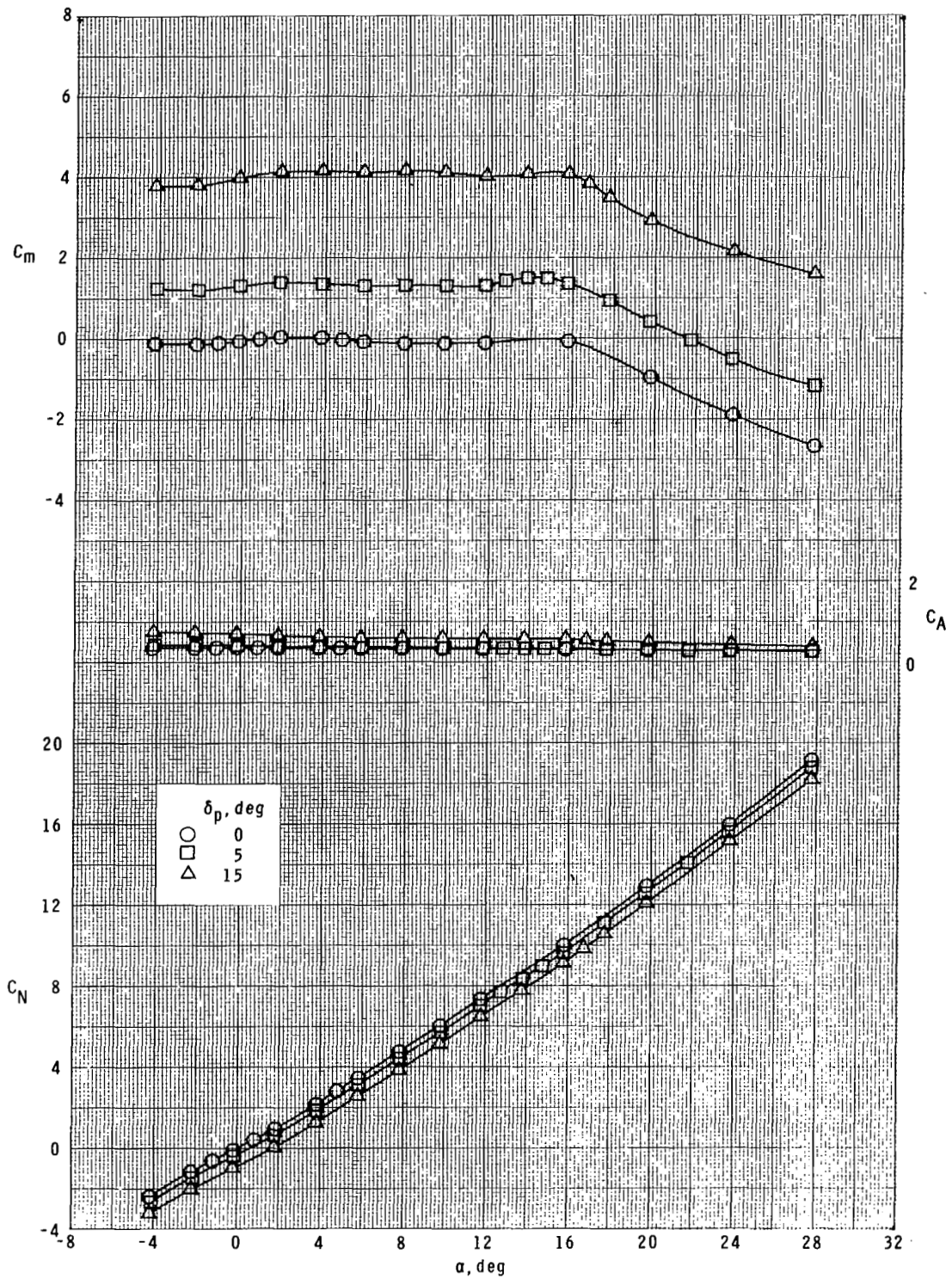
(f) Nose strake, N<sub>S</sub>.

Figure 1.- Concluded.



(a)  $M = 1.60$ .

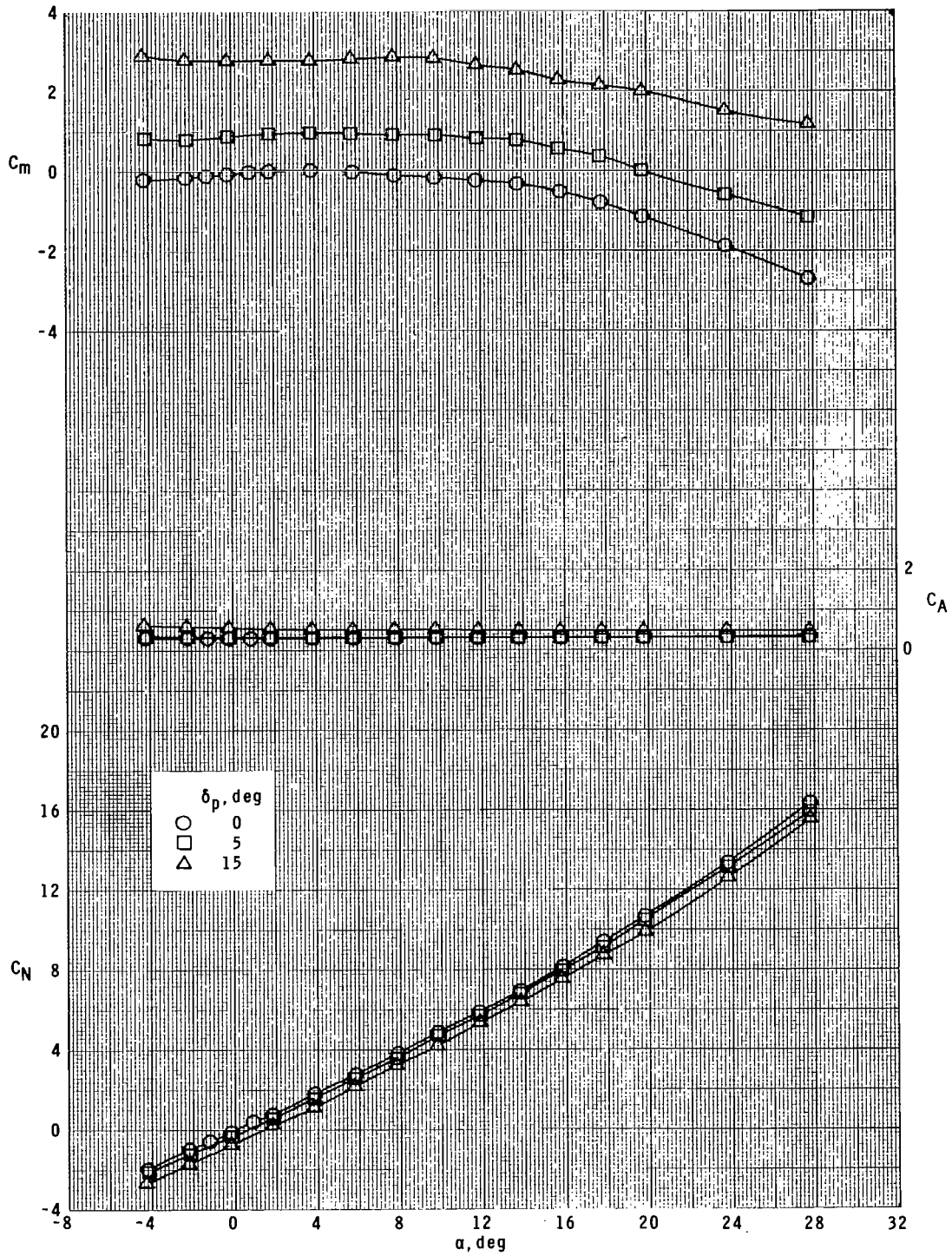
Figure 2.- Longitudinal aerodynamic characteristics for body-tail, cranked wing, nose strakes, and radar nose configuration with pitch control.



(b)  $M = 2.16$ .

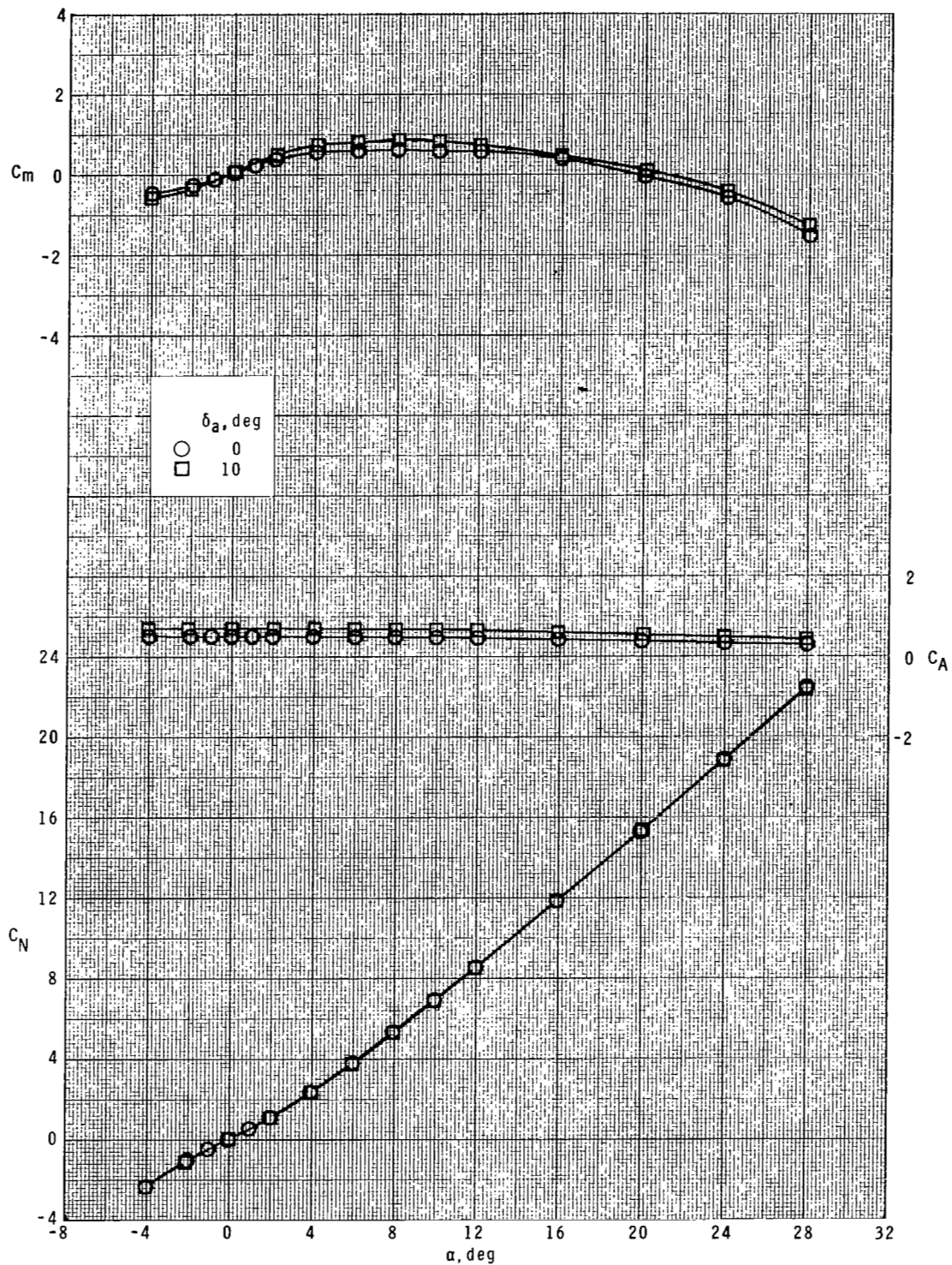
Figure 2.- Continued.





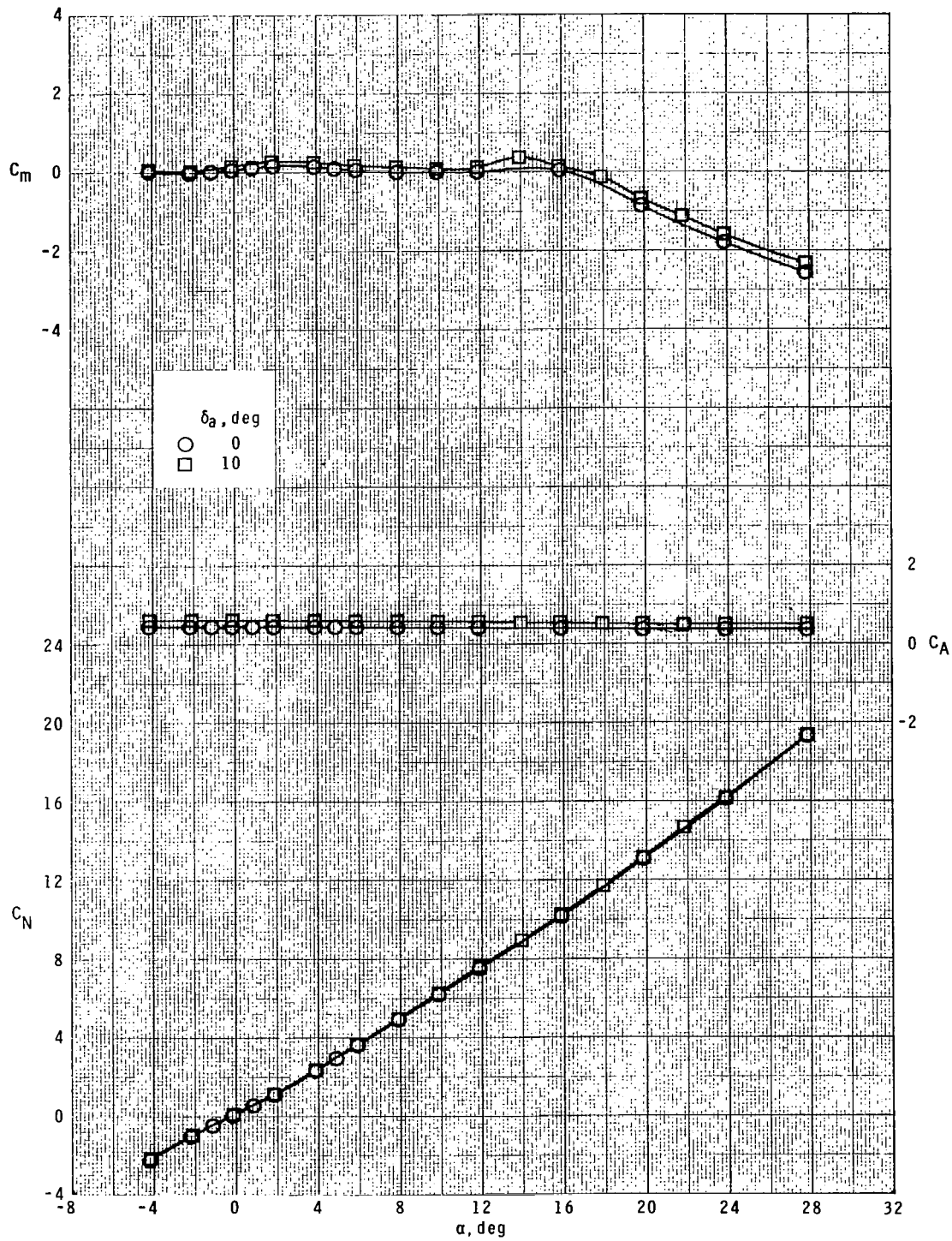
(c)  $M = 2.86$ .

Figure 2.- Concluded.



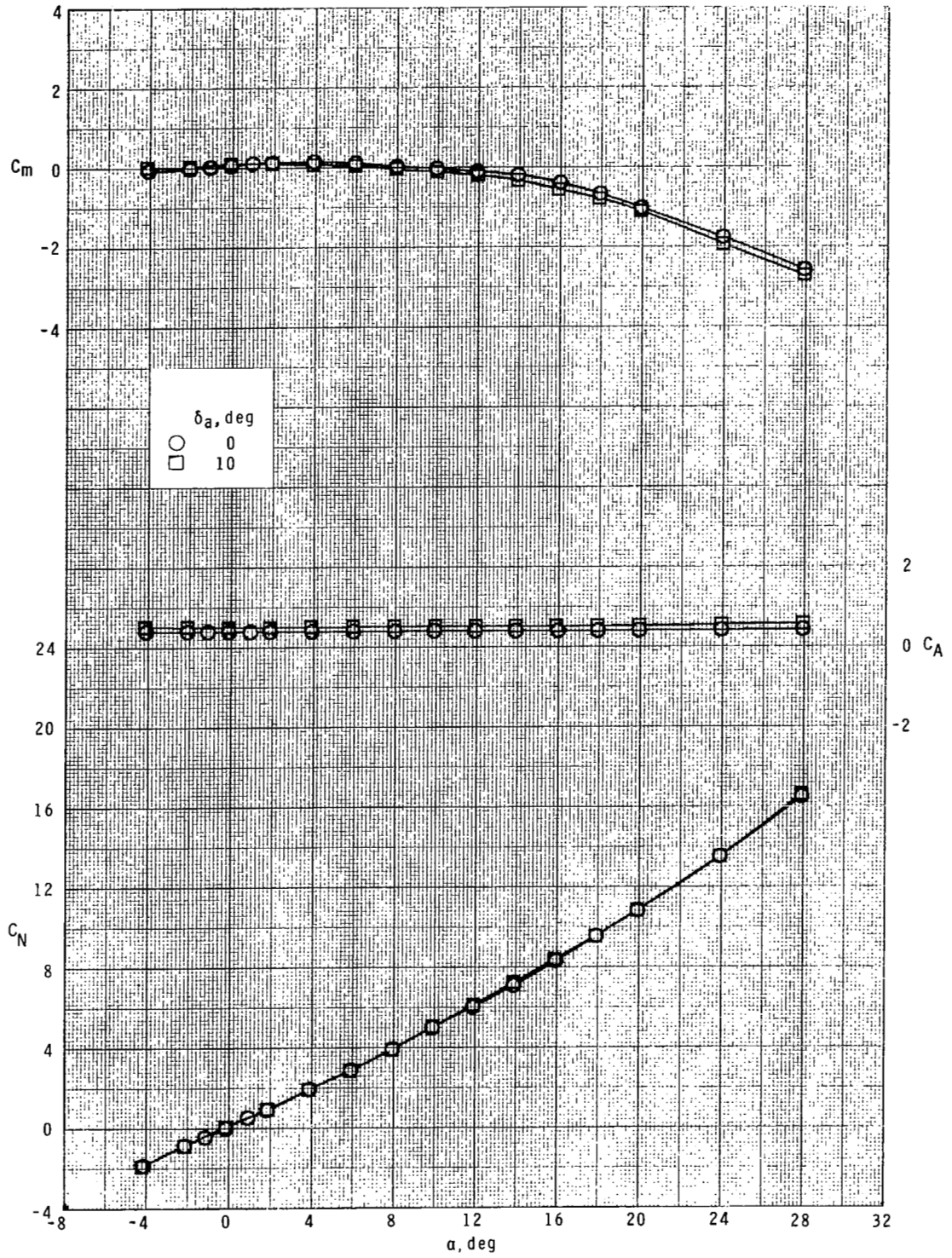
(a)  $M = 1.60$ .

Figure 3.- Longitudinal aerodynamic characteristics for body-tail, cranked wing, nose strakes, and radar nose configuration with roll control.



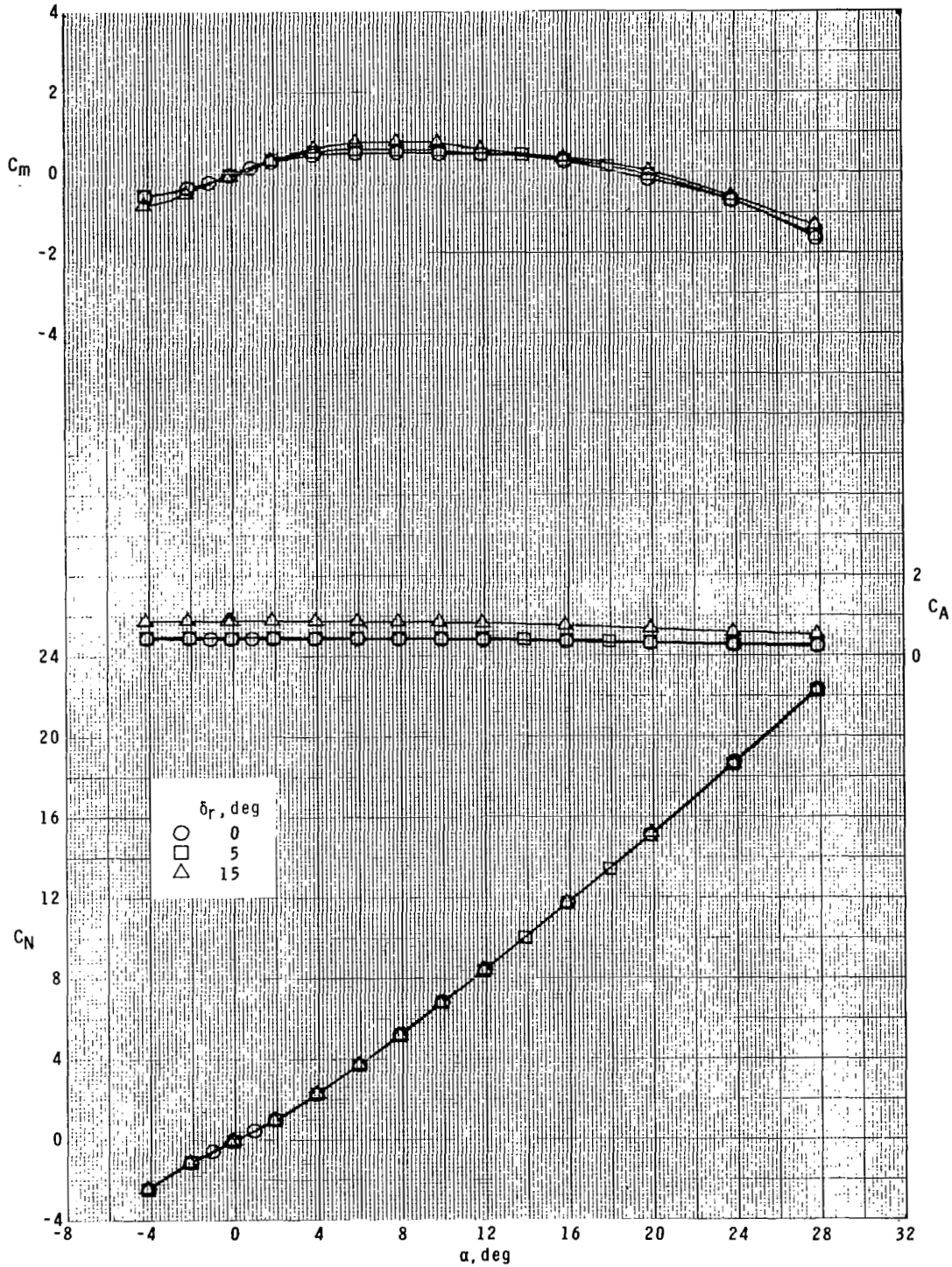
(b)  $M = 2.16$ .

Figure 3.- Continued.



(c)  $M = 2.86$ .

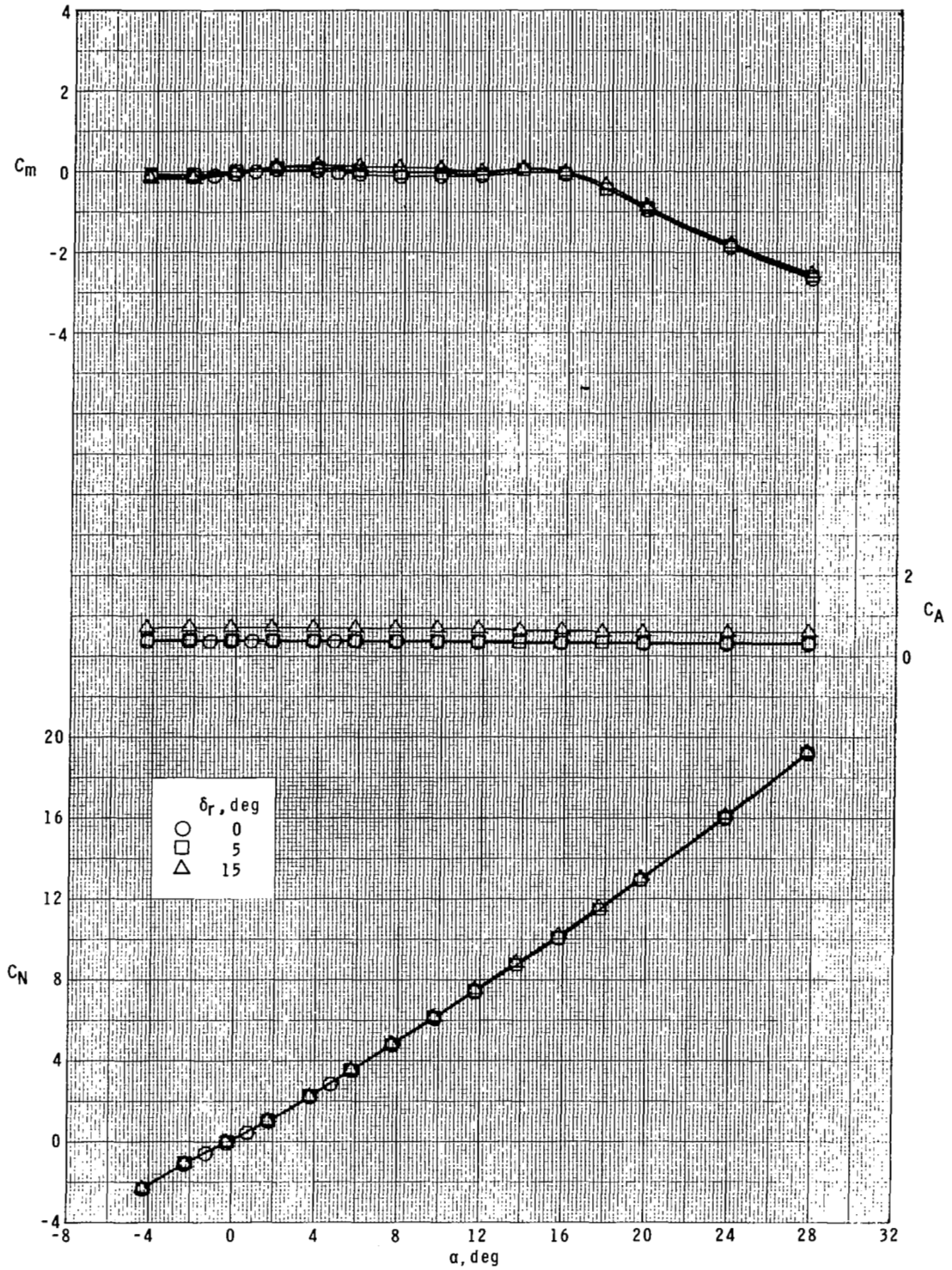
Figure 3.- Concluded.



(a)  $M = 1.60$ .

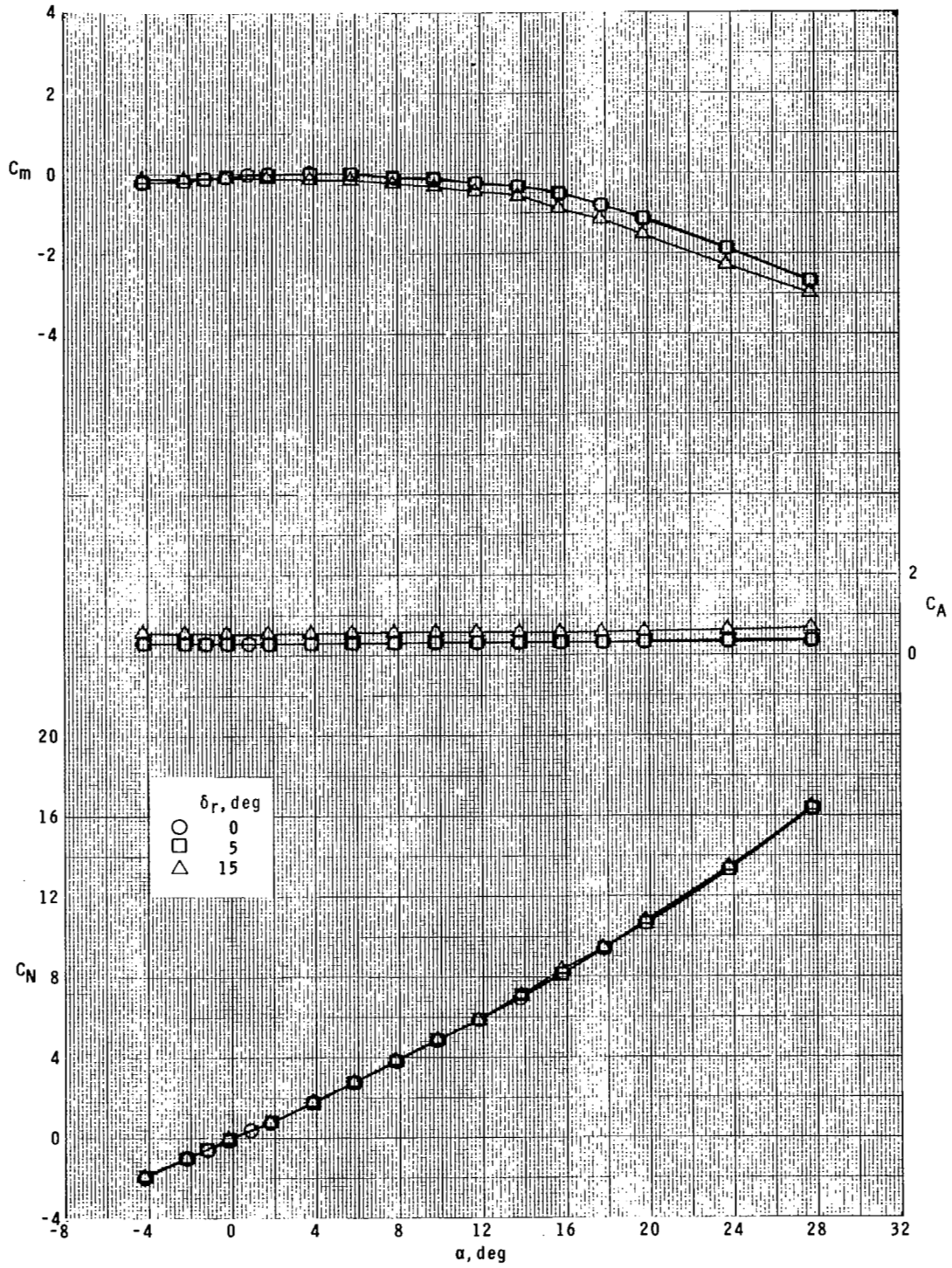
Figure 4.- Longitudinal aerodynamic characteristics for body-tail, cranked wing, nose strakes, and radar nose configuration with yaw control.





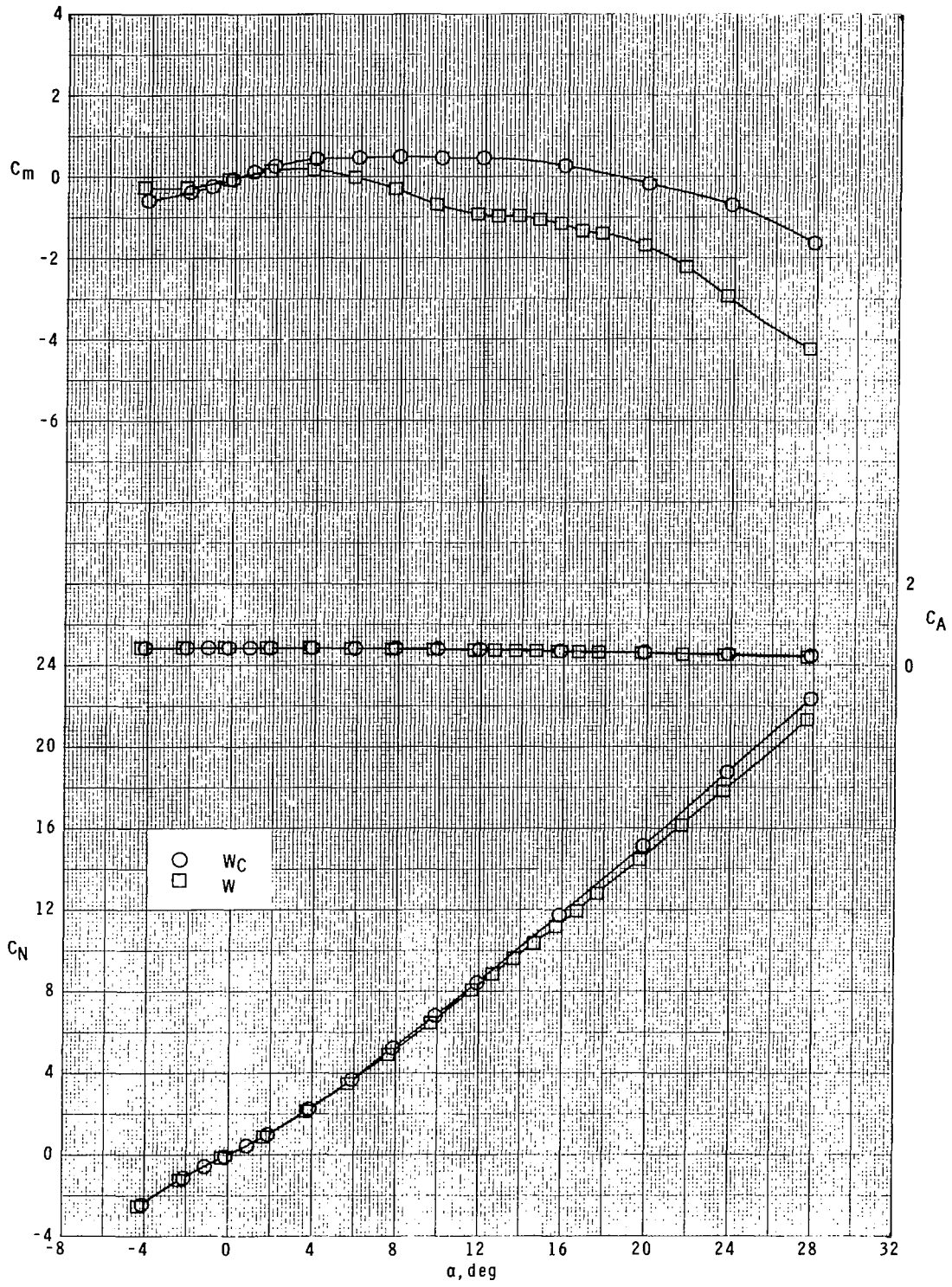
(b)  $M = 2.16$ .

Figure 4.- Continued.



(c)  $M = 2.86$ .

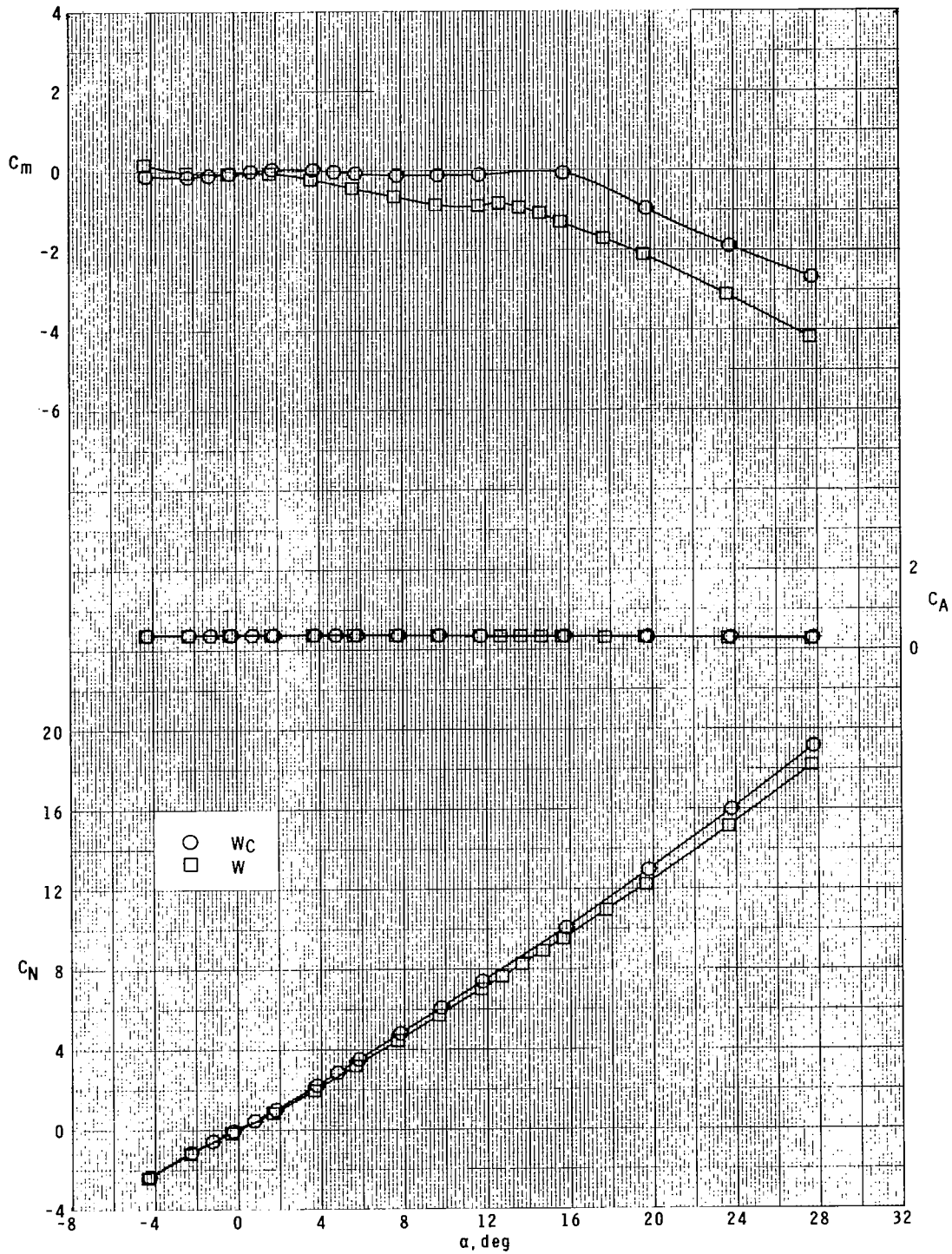
Figure 4.- Concluded.



(a)  $M = 1.60$ .

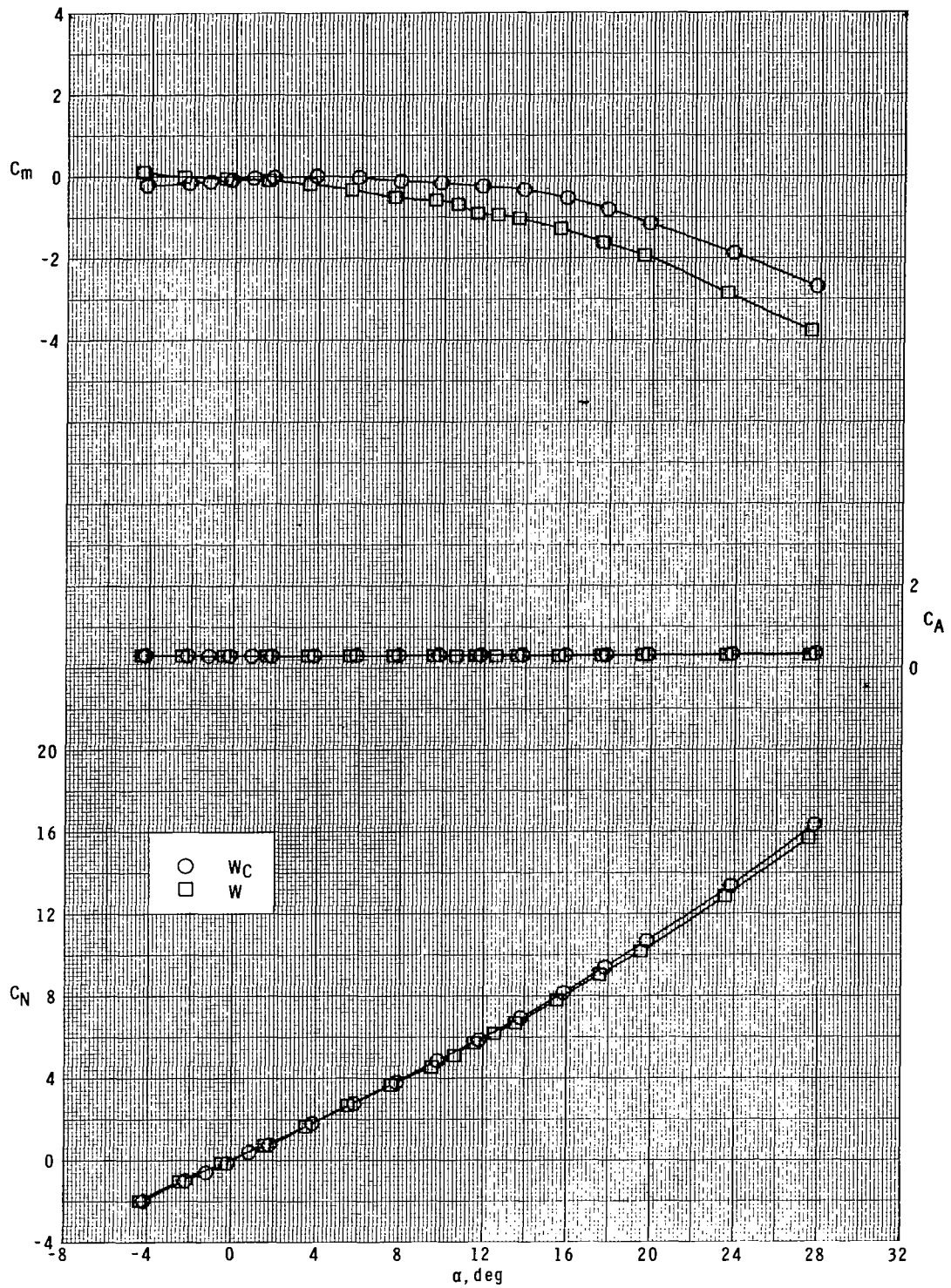
Figure 5.- Effect of wing planform shape on longitudinal aerodynamic characteristics for body-tail, nose strakes, and radar nose configuration.





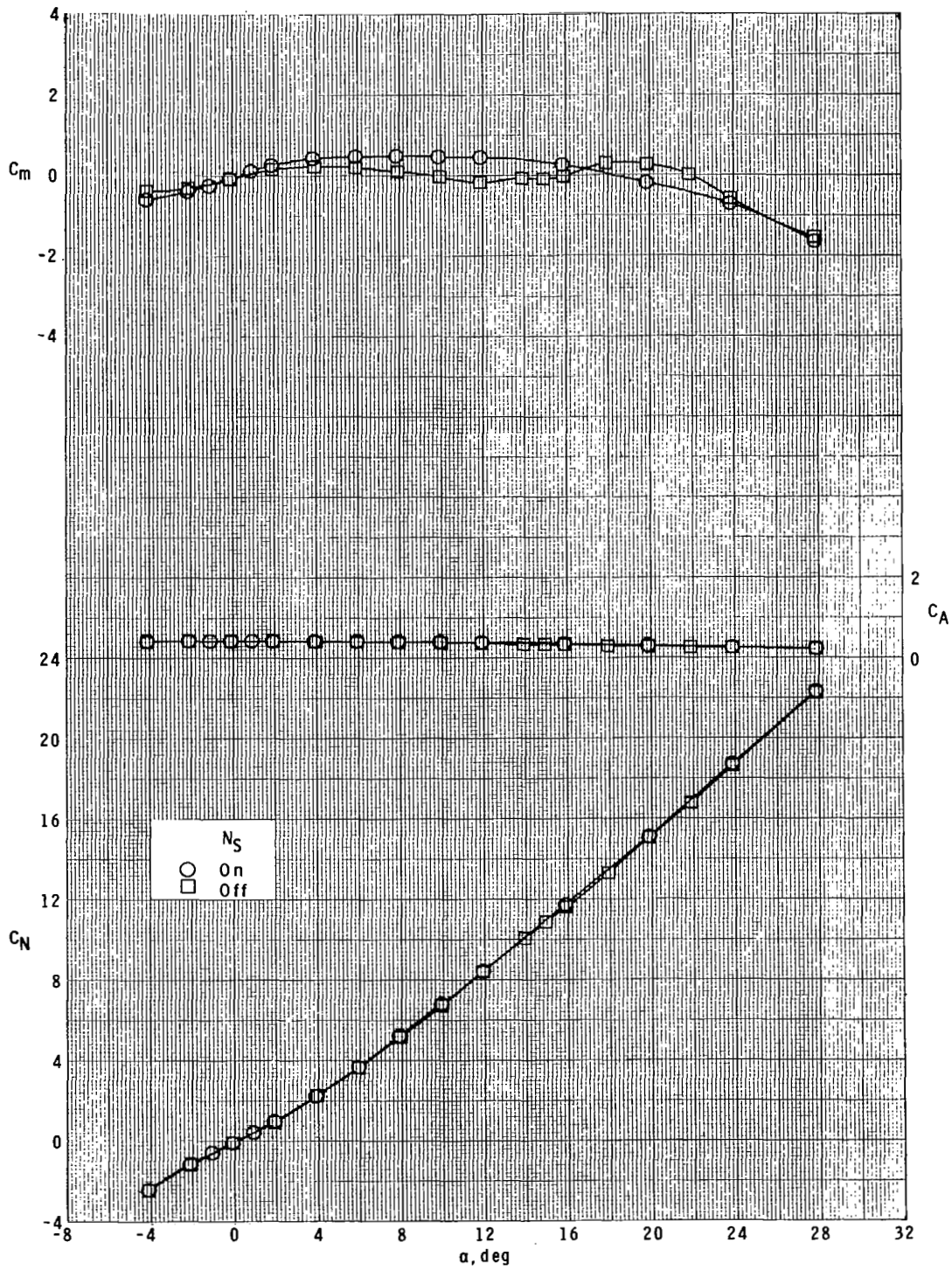
(b)  $M = 2.16$ .

Figure 5.- Continued.



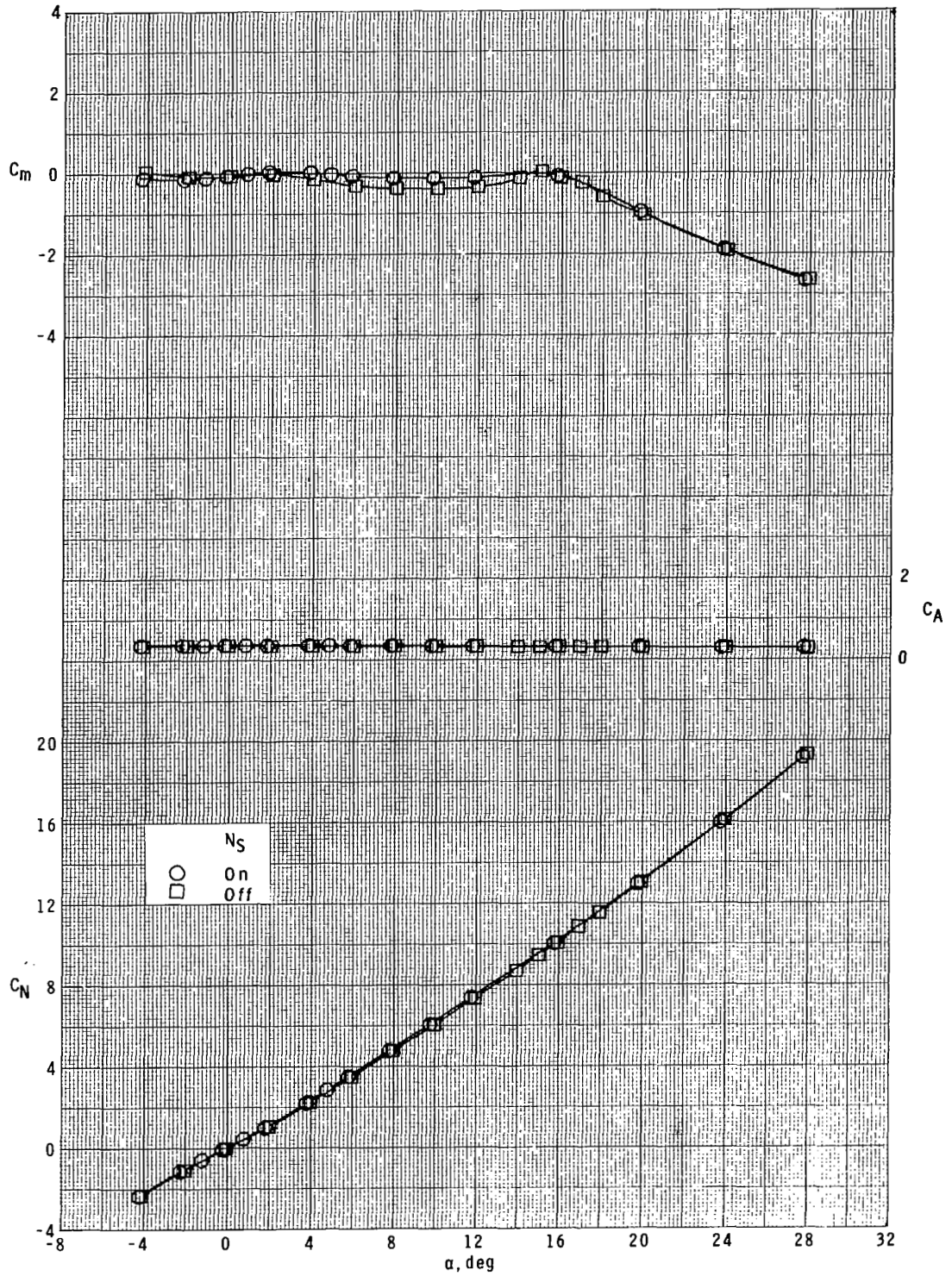
(c)  $M = 2.86$ .

Figure 5.- Concluded.



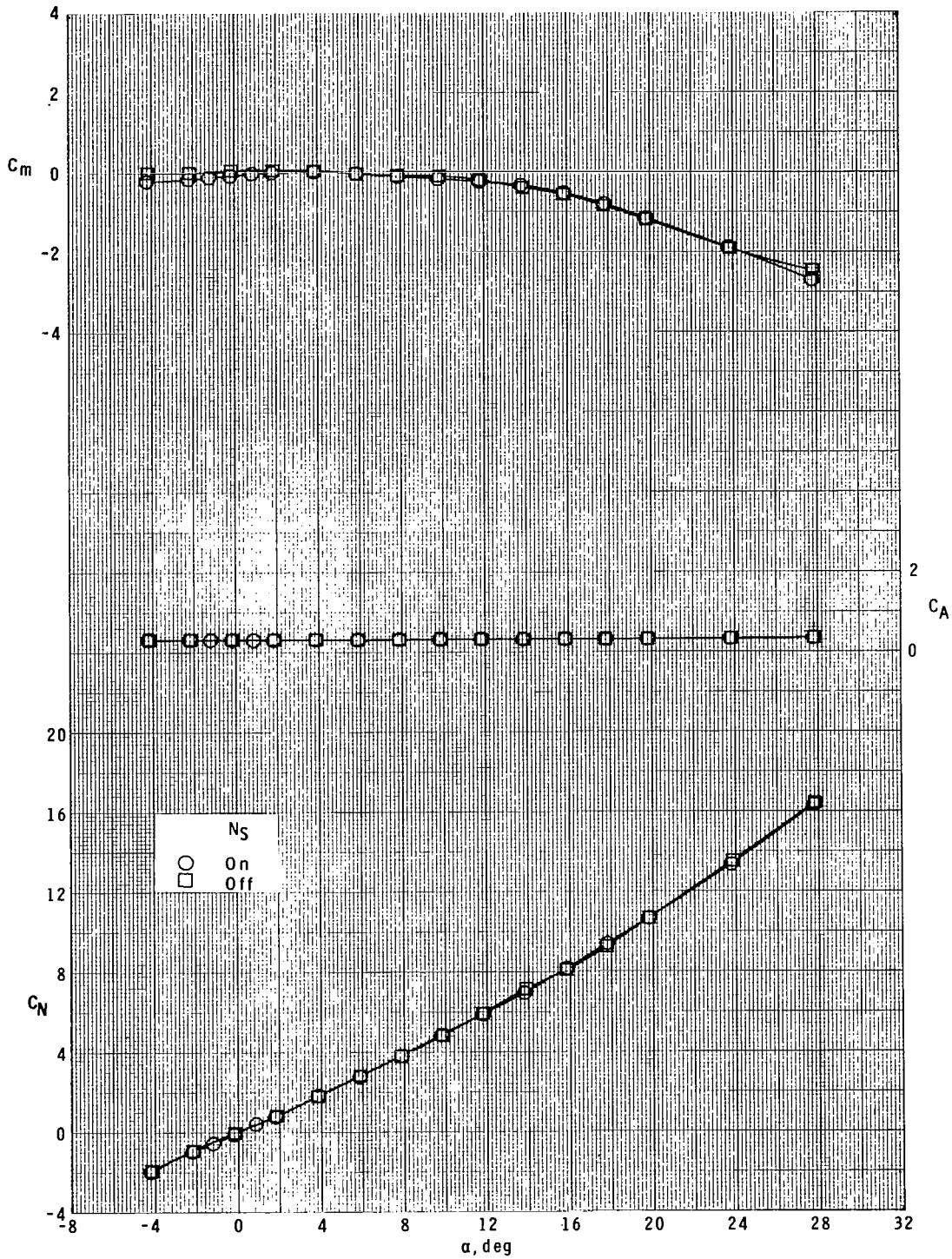
(a)  $M = 1.60$ .

Figure 6.- Effect of nose strakes on longitudinal aerodynamic characteristics for body-tail, cranked wing, and radar nose configuration.



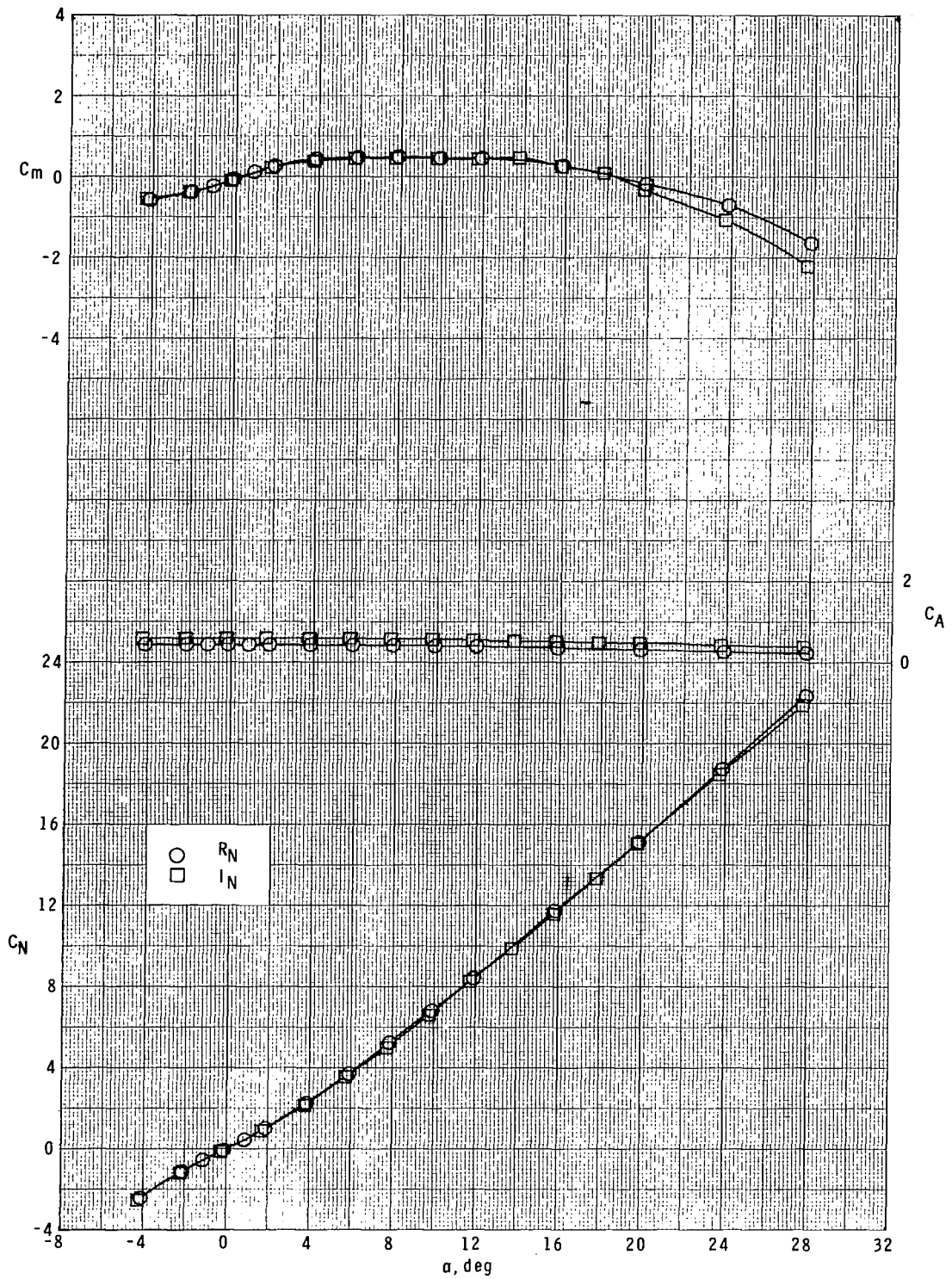
(b)  $M = 2.16$ .

Figure 6.- Continued.



(c)  $M = 2.86$ .

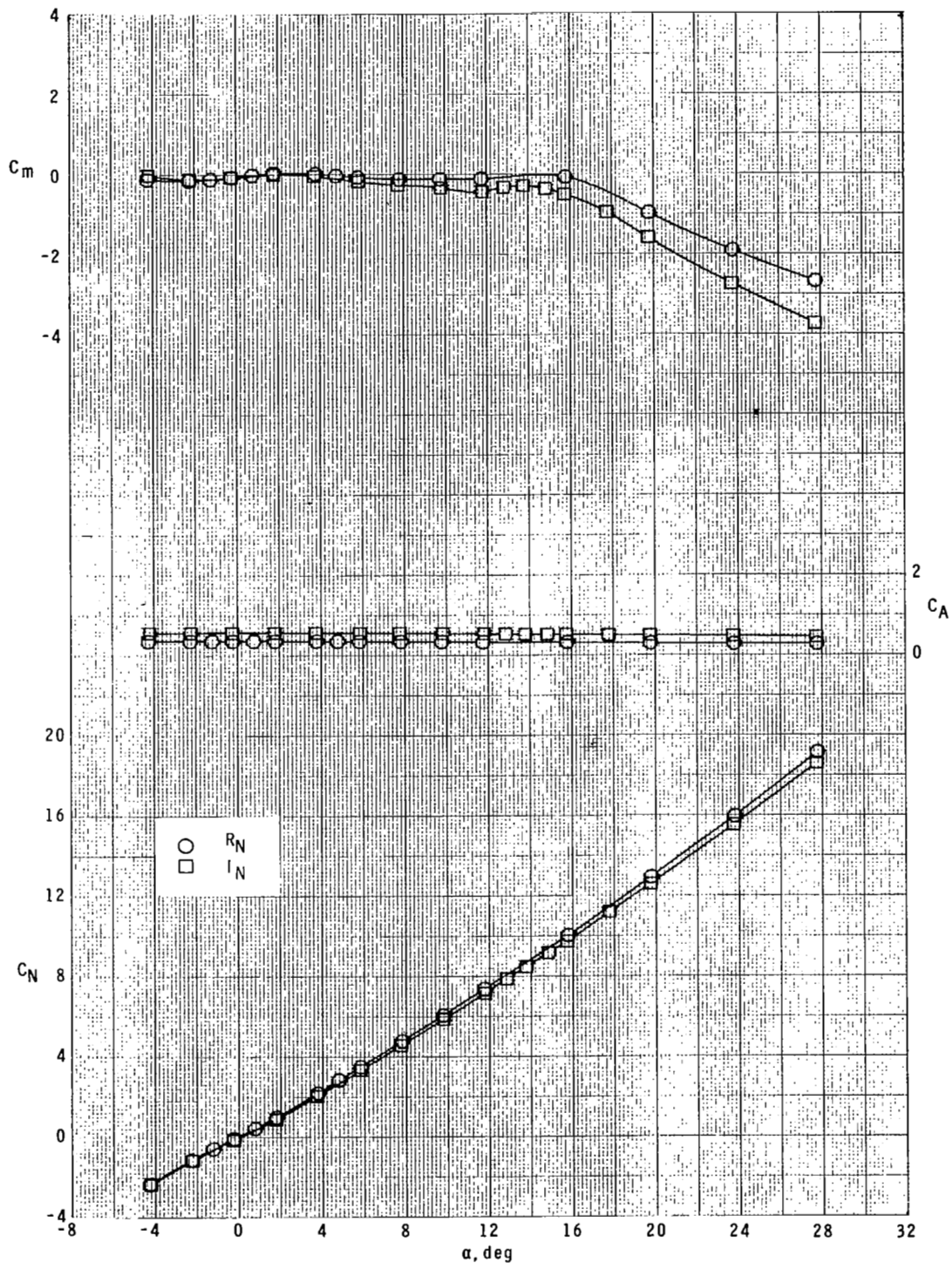
Figure 6.- Concluded.



(a)  $M = 1.60$ .

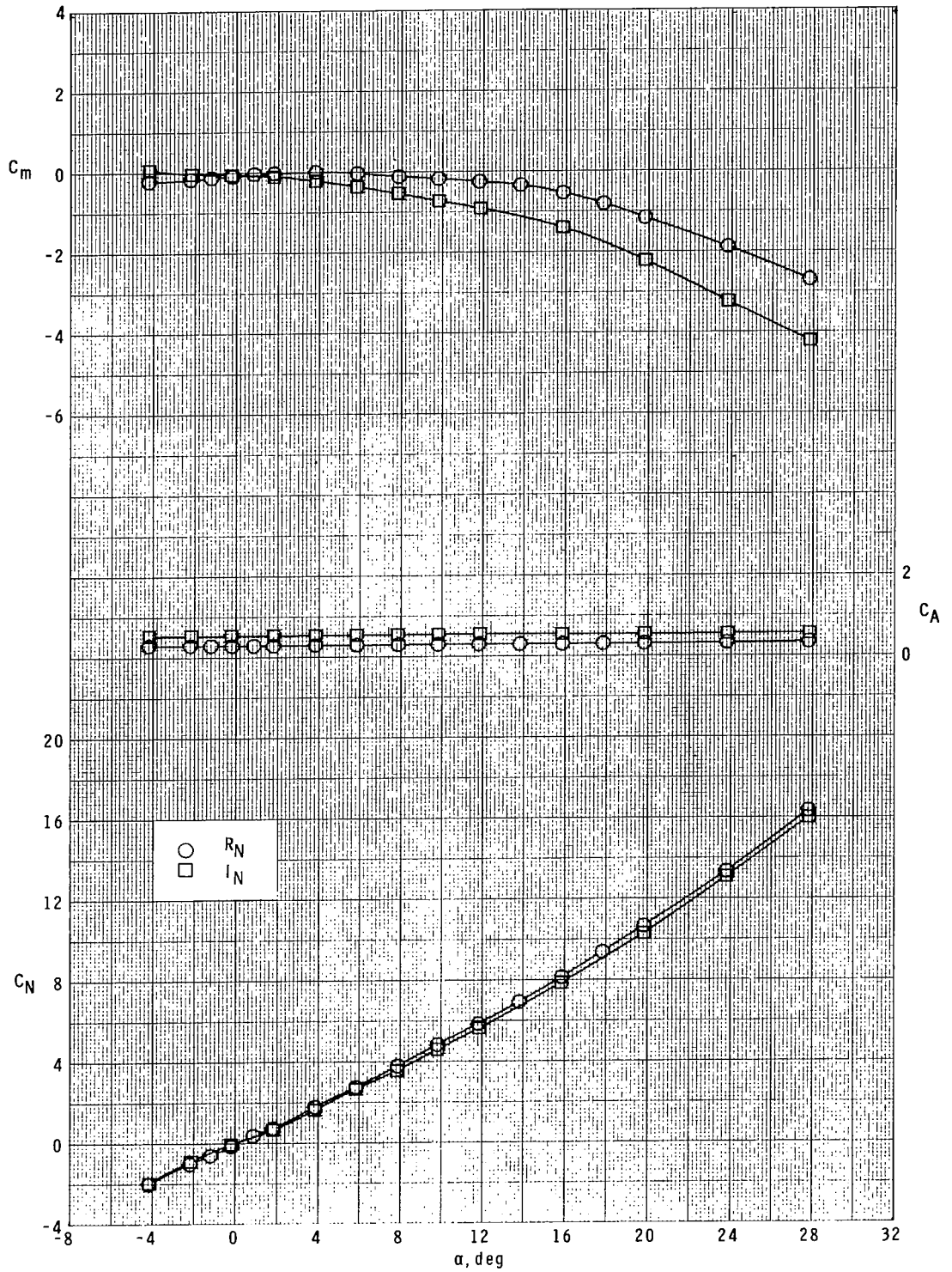
Figure 7.- Effect of nose shape on longitudinal aerodynamic characteristics for body-tail<sub>1</sub>, cranked wing, and nose strakes configuration.





(b)  $M = 2.16$ .

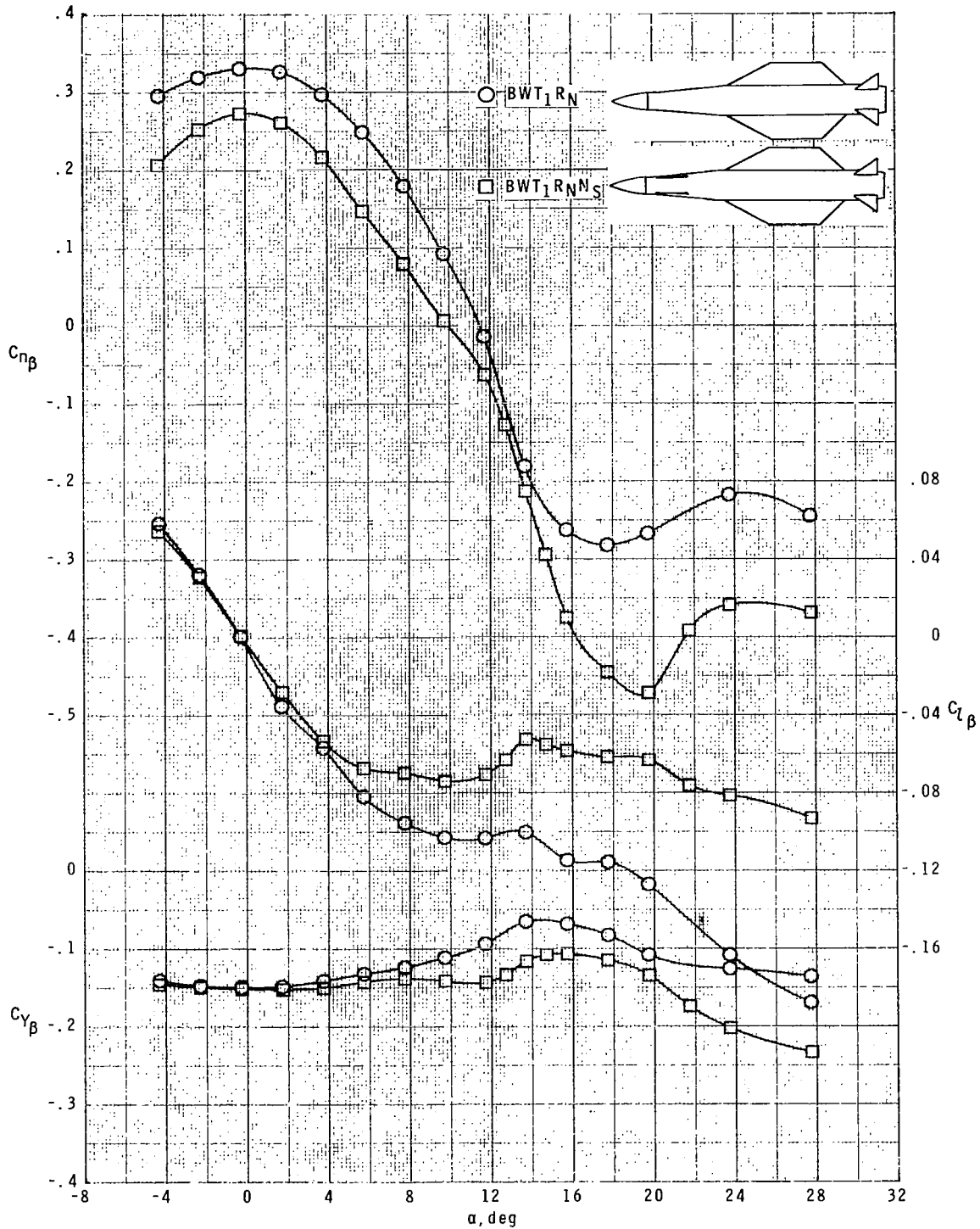
Figure 7.- Continued.



(c)  $M = 2.86$ .

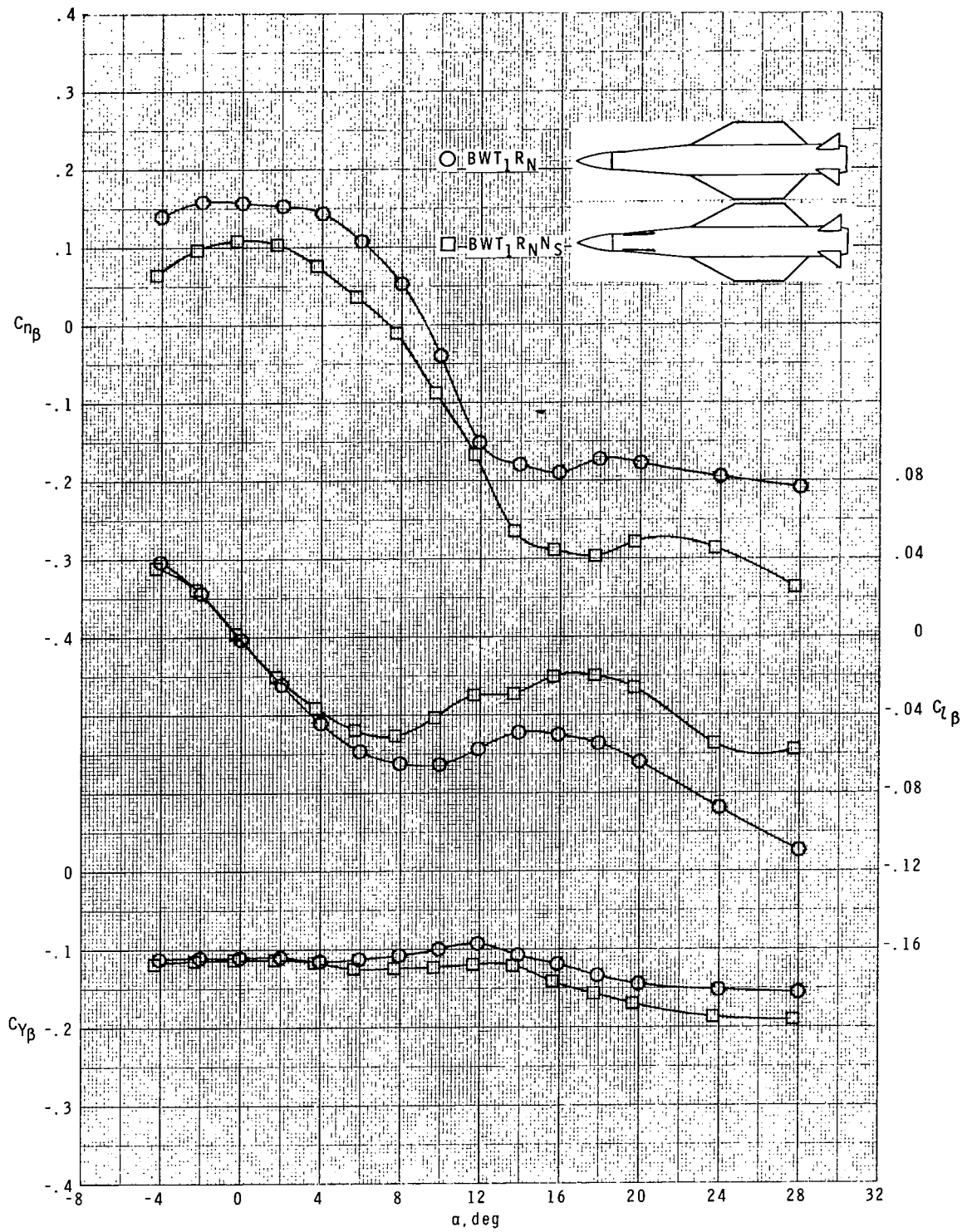
Figure 7.- Concluded.





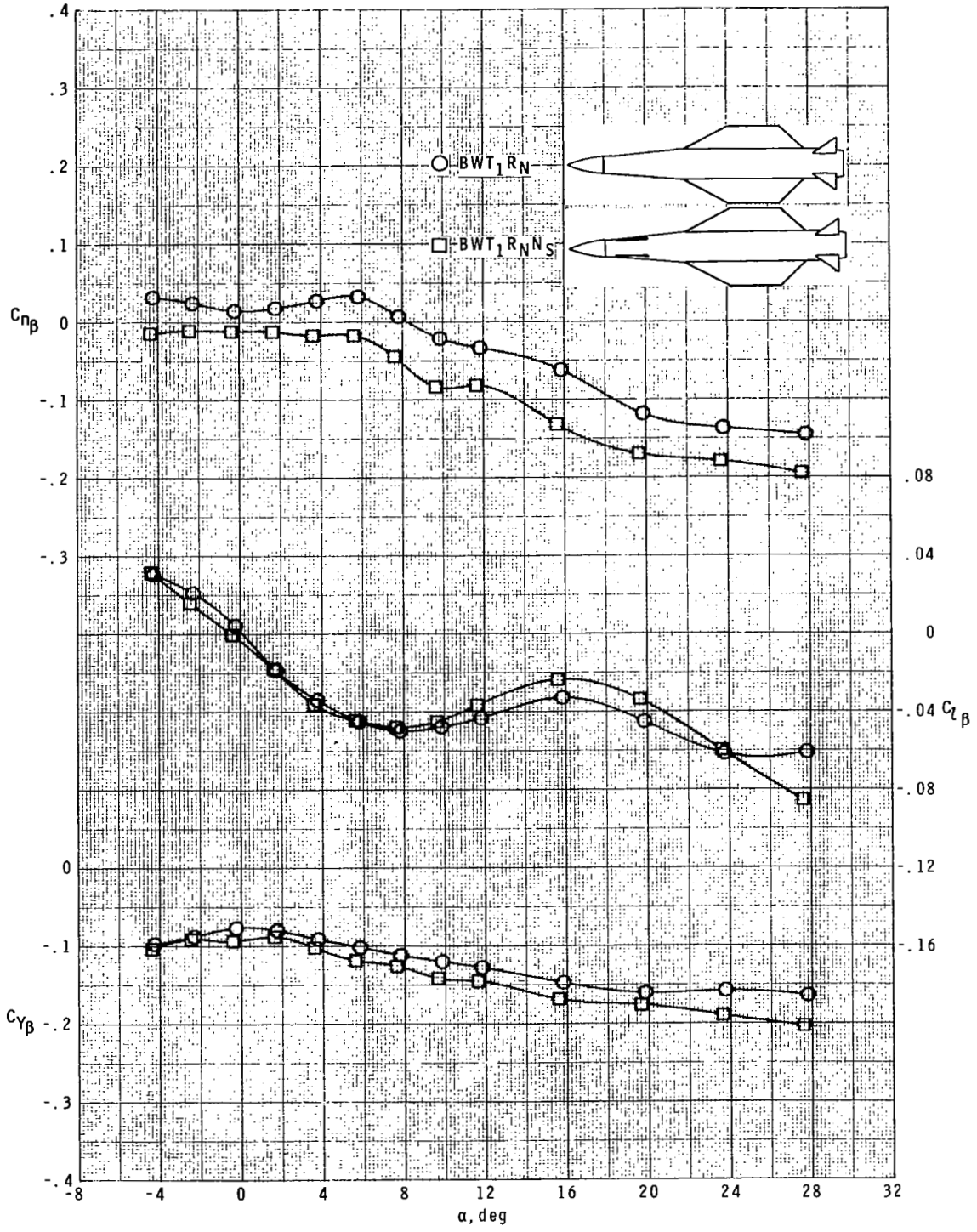
(a)  $M = 1.60$ .

Figure 8.- Effect of nose strakes on lateral-directional characteristics for straight wing configuration.



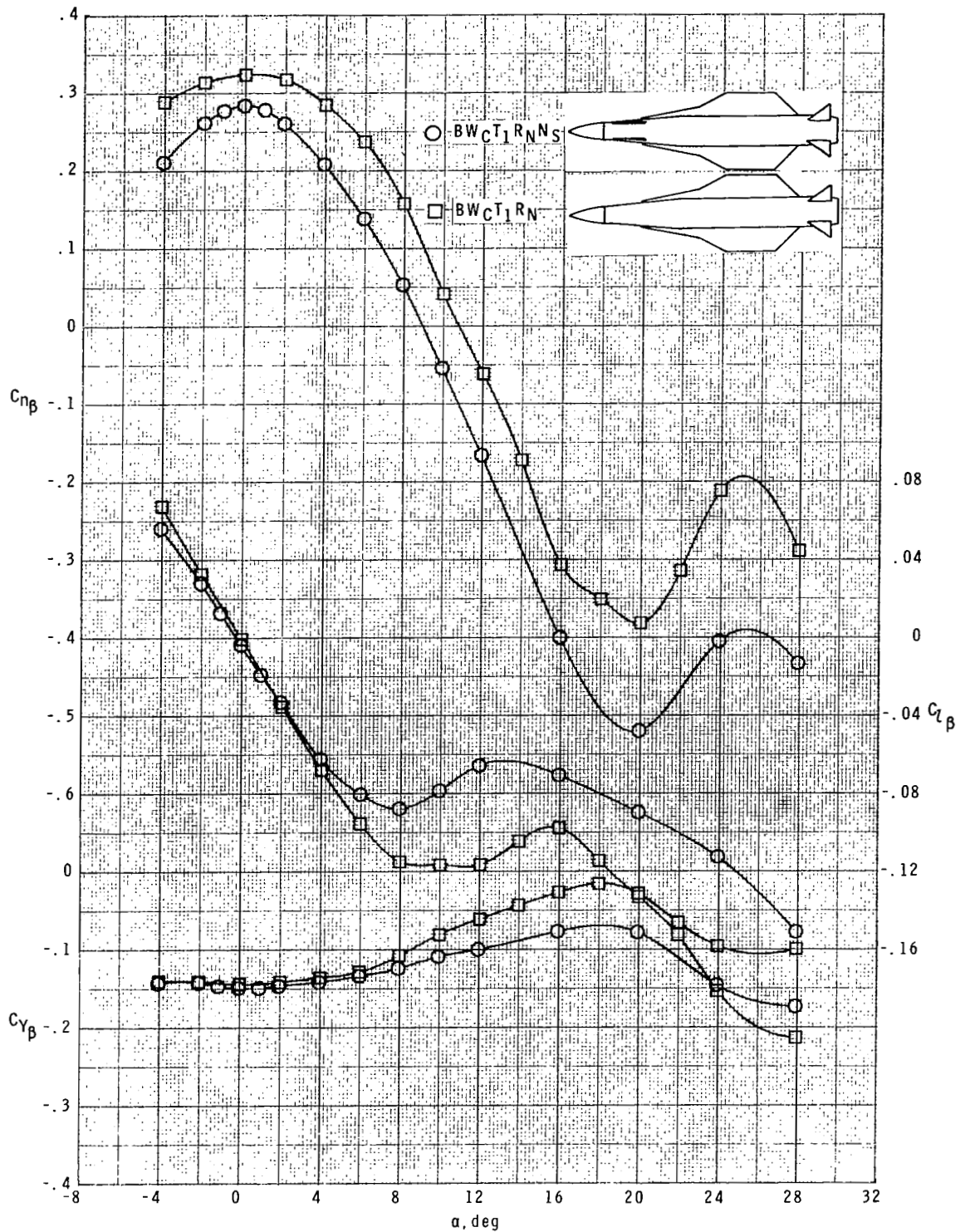
(b)  $M = 2.16$ .

Figure 8.- Continued.



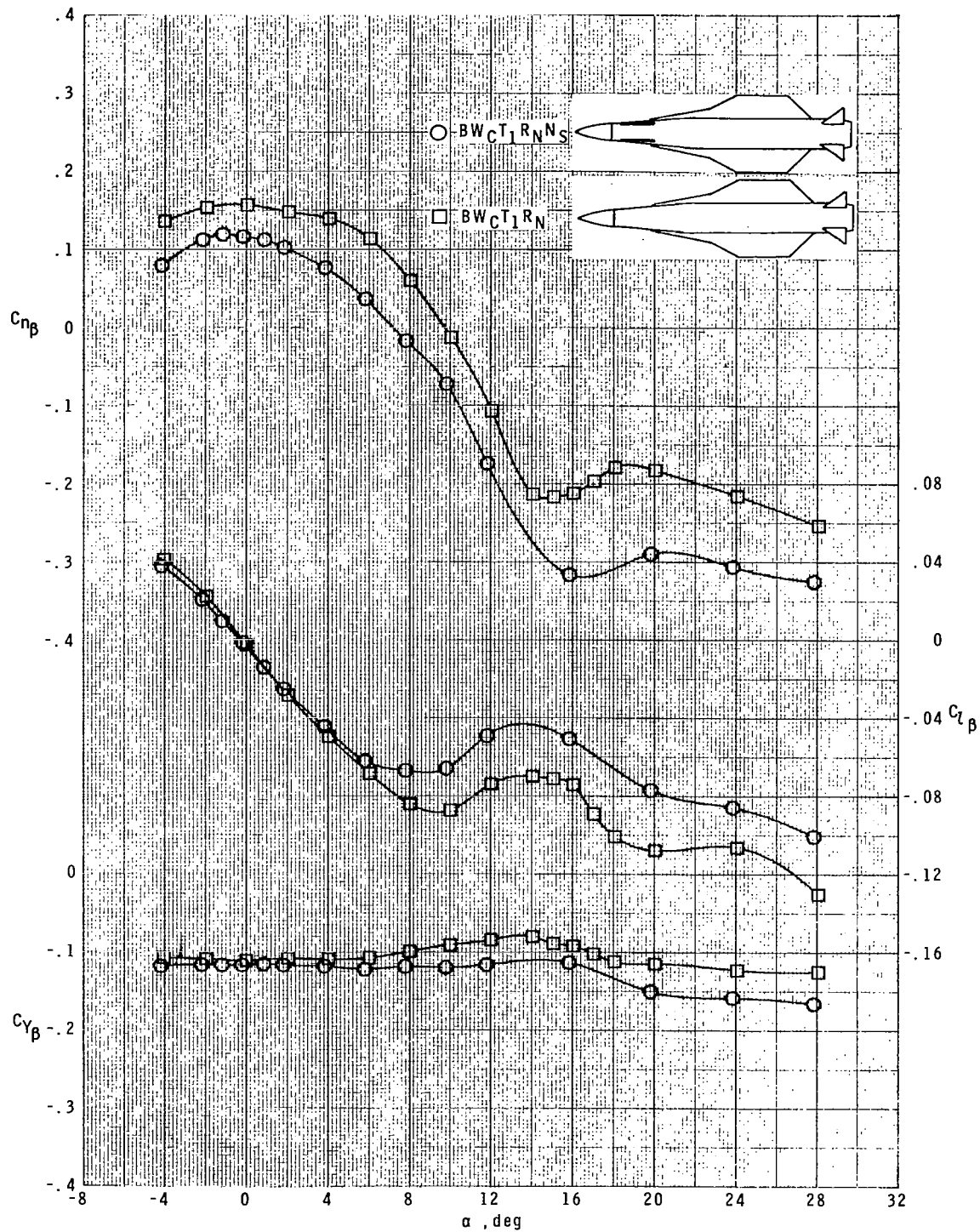
(c)  $M = 2.86$ .

Figure 8.- Concluded.



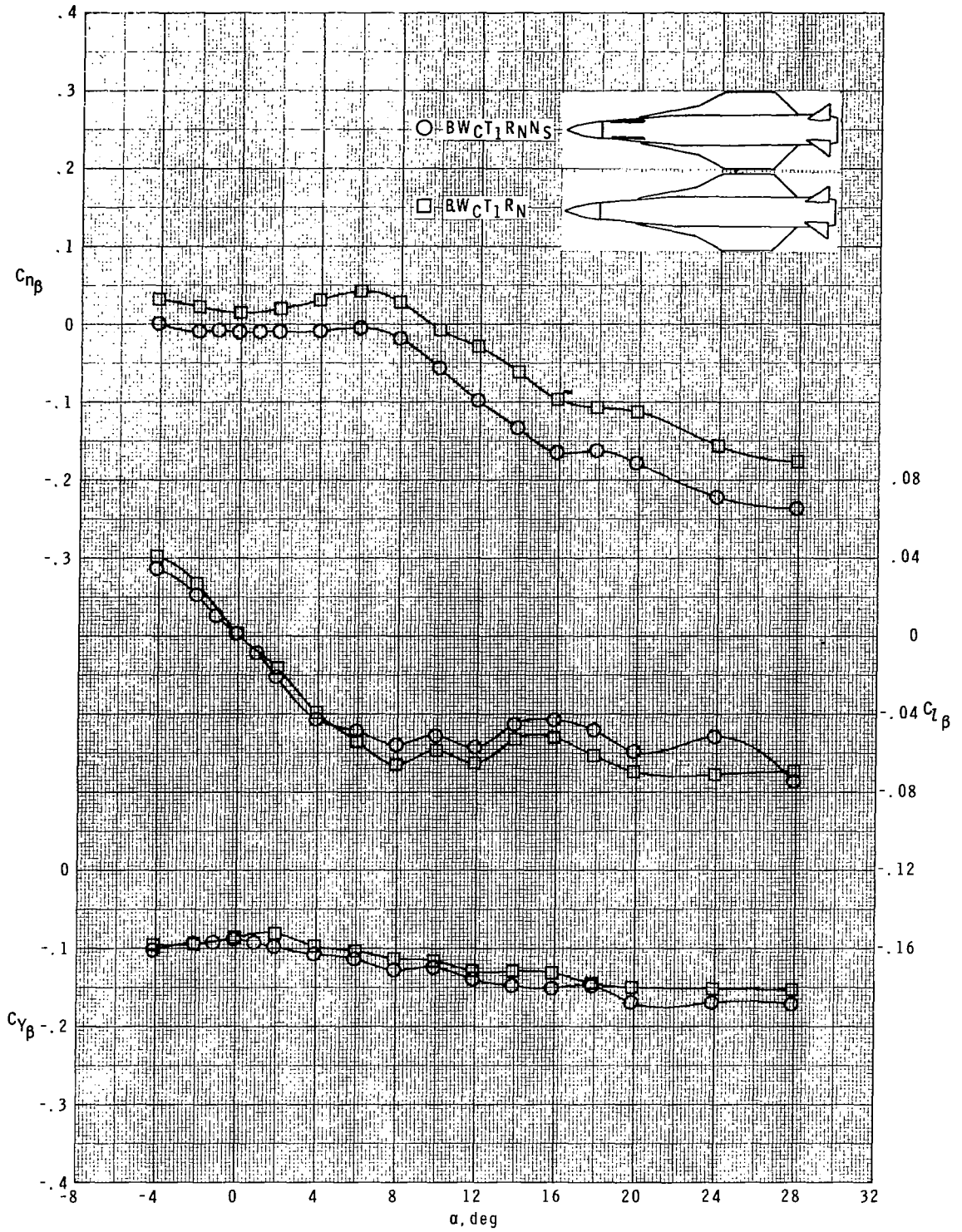
(a)  $M = 1.60$ .

Figure 9.- Effect of nose strakes on lateral-directional characteristics for cranked wing configuration.



(b)  $M = 2.16$ .

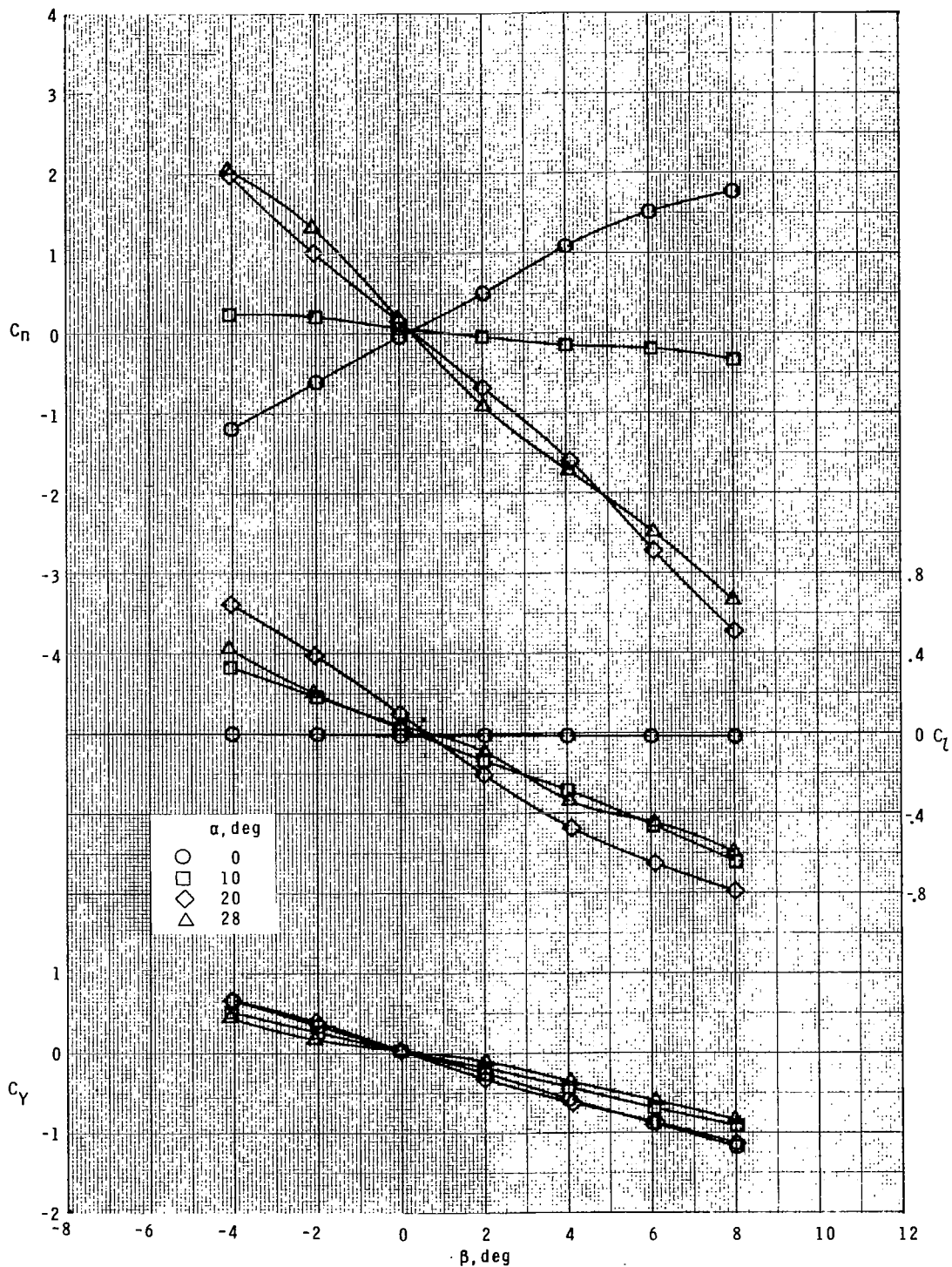
Figure 9.- Continued.



(c)  $M = 2.86$ .

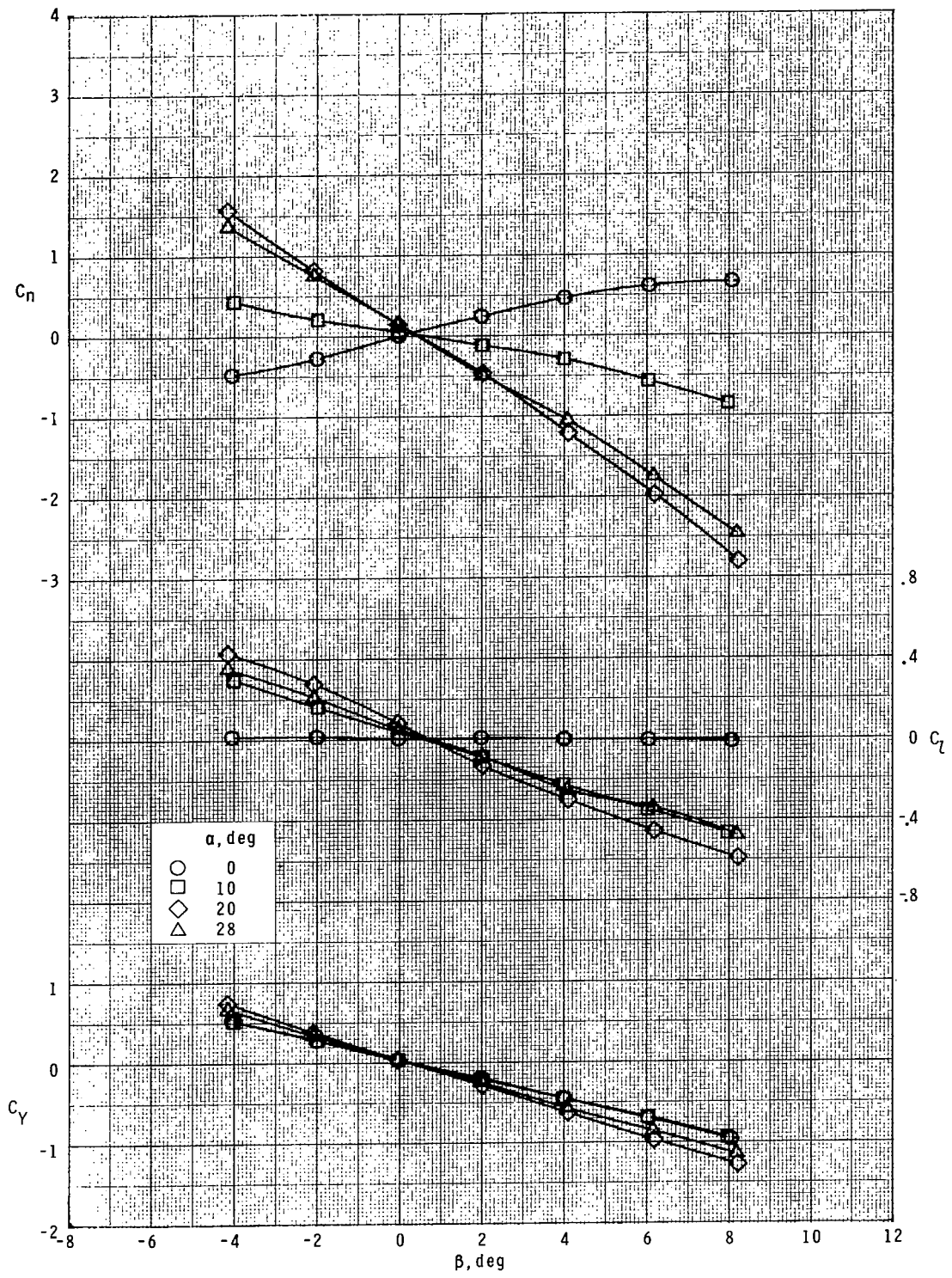
Figure 9.- Concluded.





(a)  $M = 1.60$ .

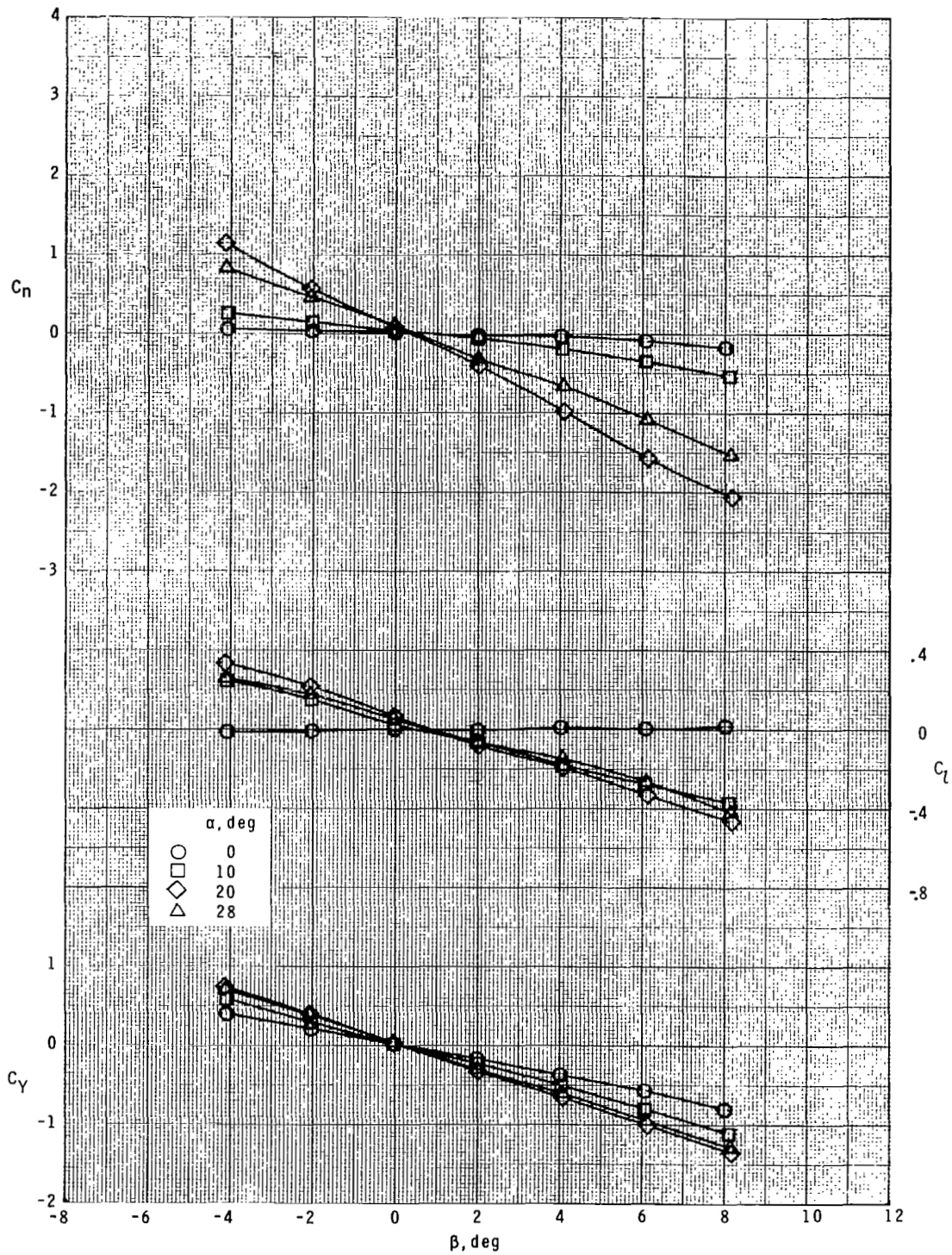
Figure 10.- Directional stability characteristics for body-tail, cranked wing, nose strakes, and radar nose configuration in sideslip at angle of attack.



(b)  $M = 2.16$ .

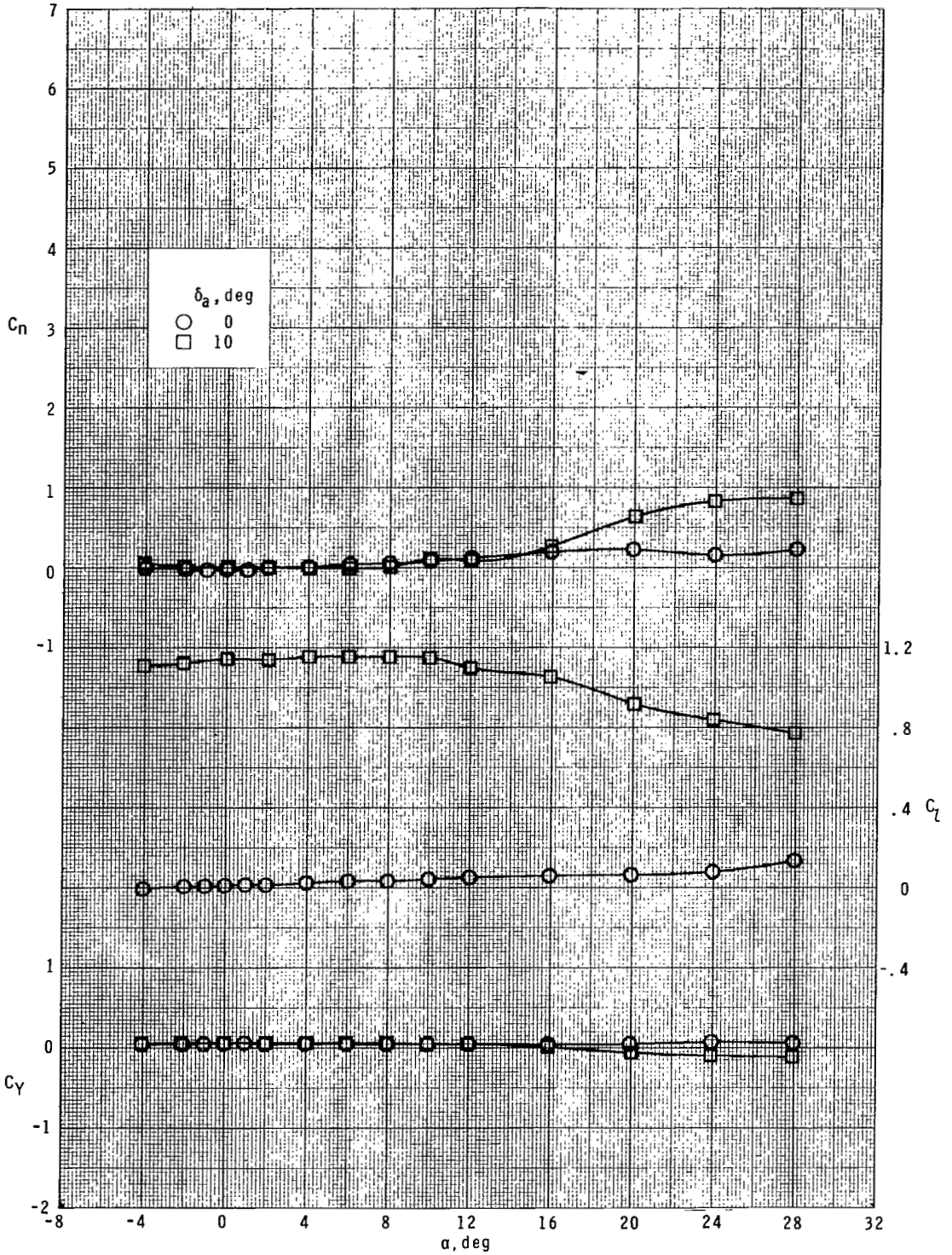
Figure 10.- Continued.





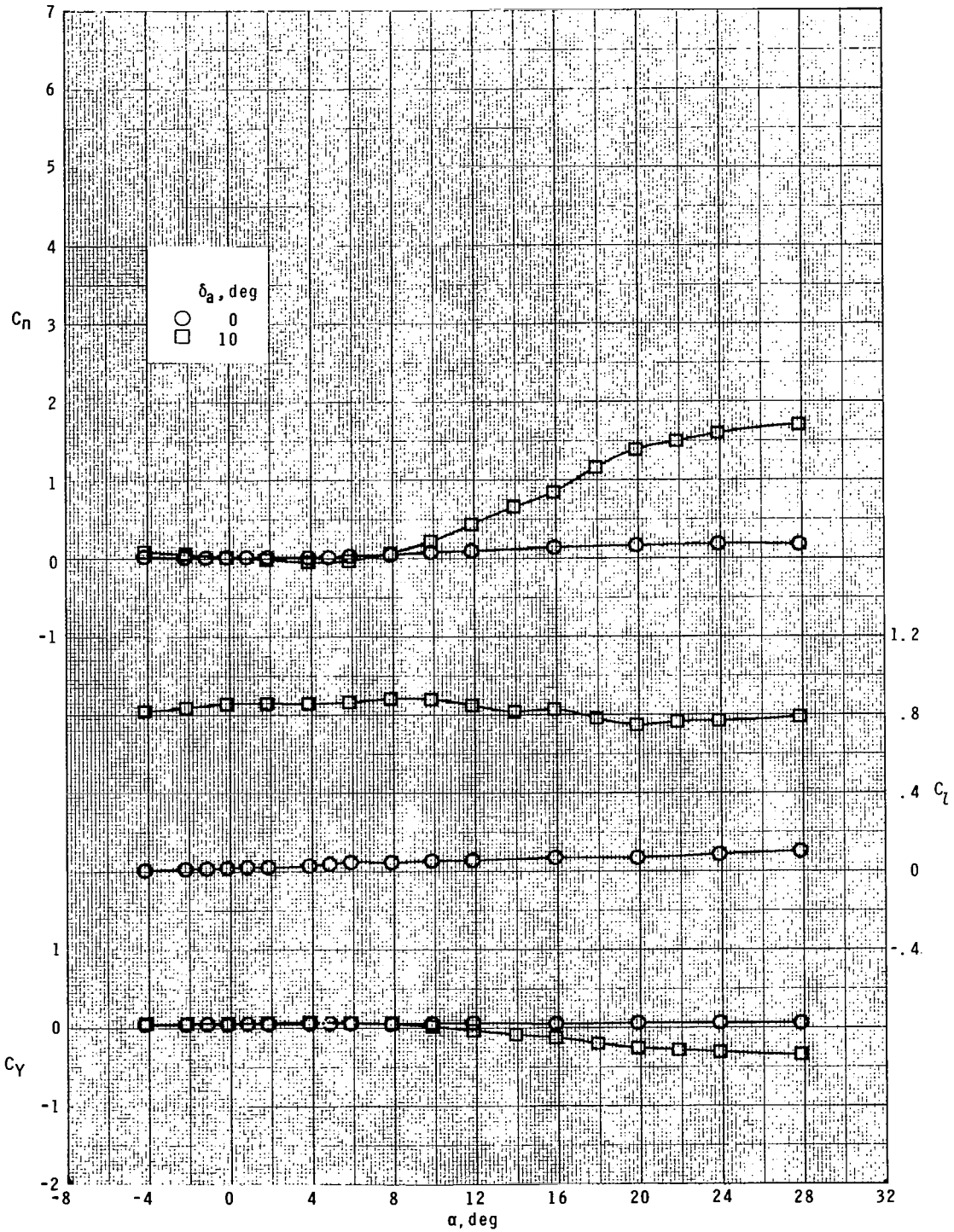
(c)  $M = 2.86$ .

Figure 10.- Concluded.



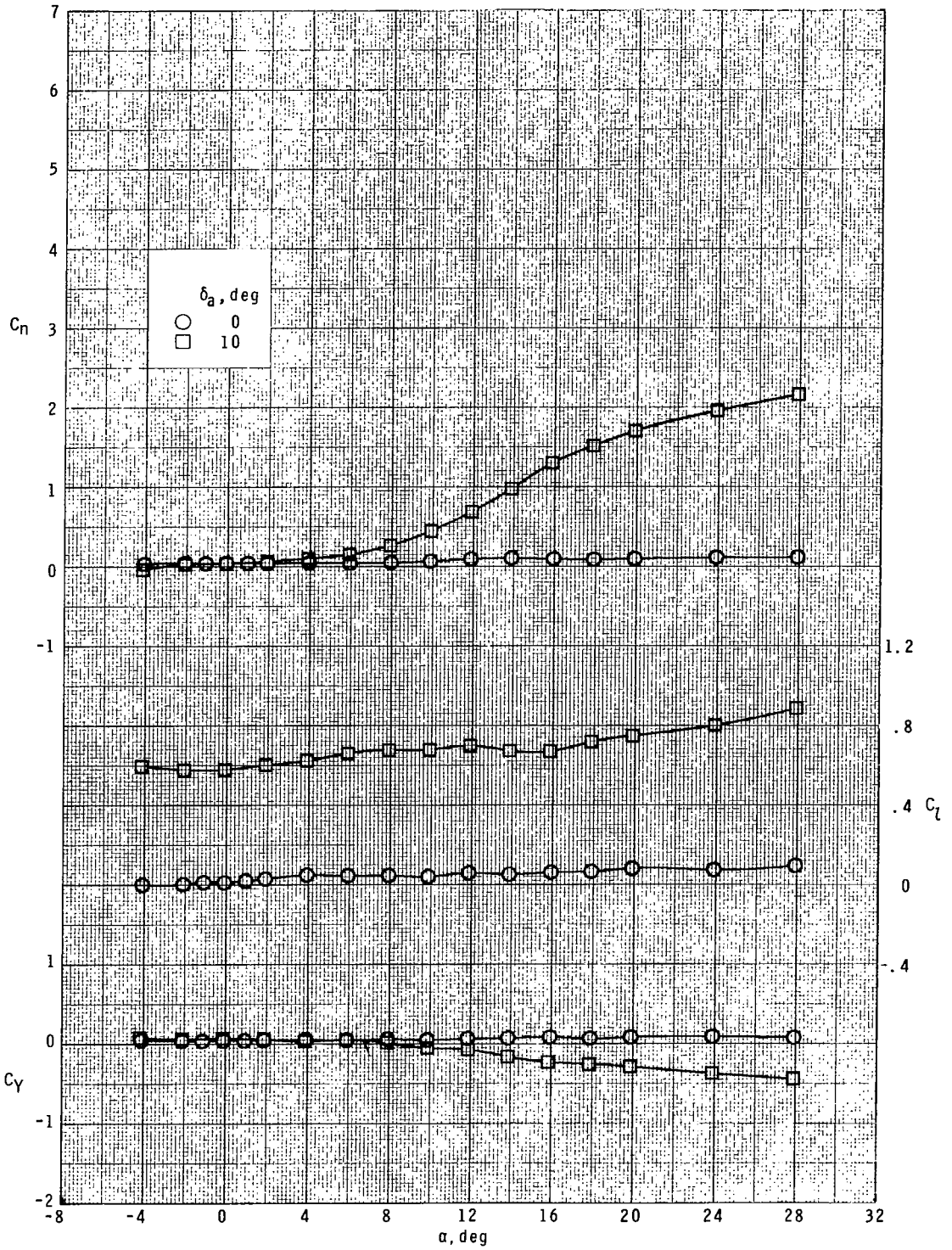
(a)  $M = 1.60$ .

Figure 11.- Roll control characteristics for body-tail<sub>1</sub>, cranked wing, nose strakes, and radar nose configuration.



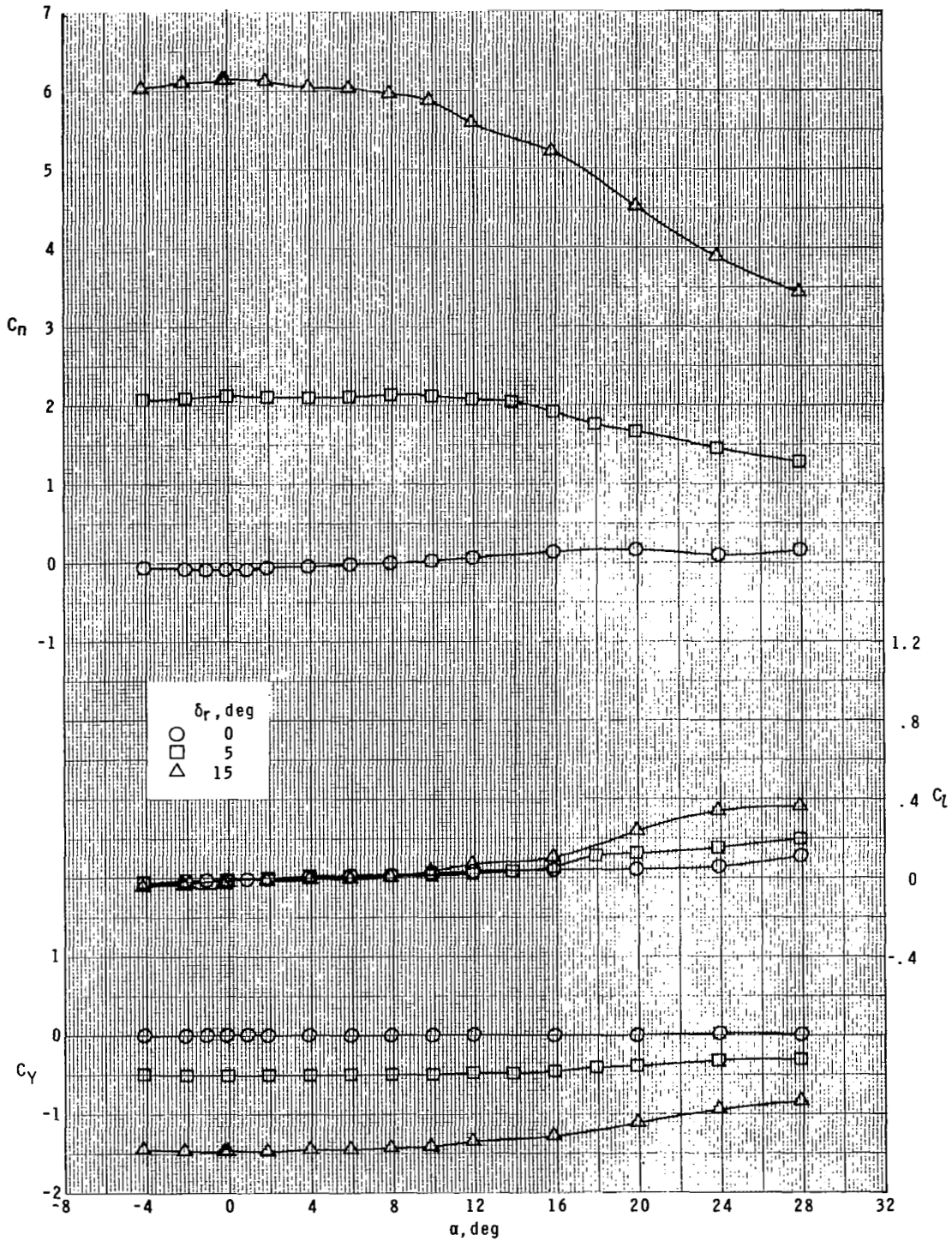
(b)  $M = 2.16$ .

Figure 11.- Continued.



(c)  $M = 2.86$ .

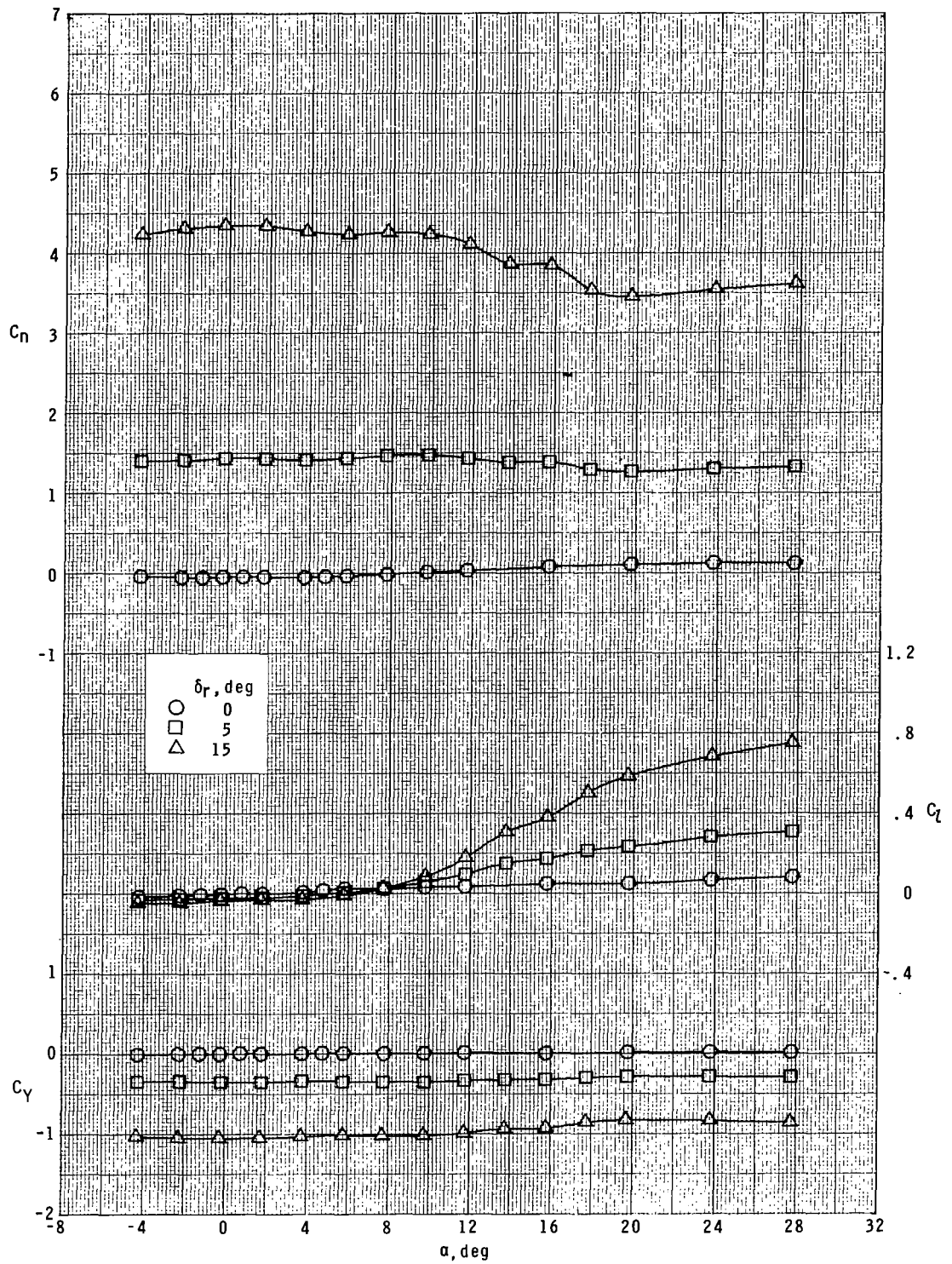
Figure 11.- Concluded.



(a)  $M = 1.60$ .

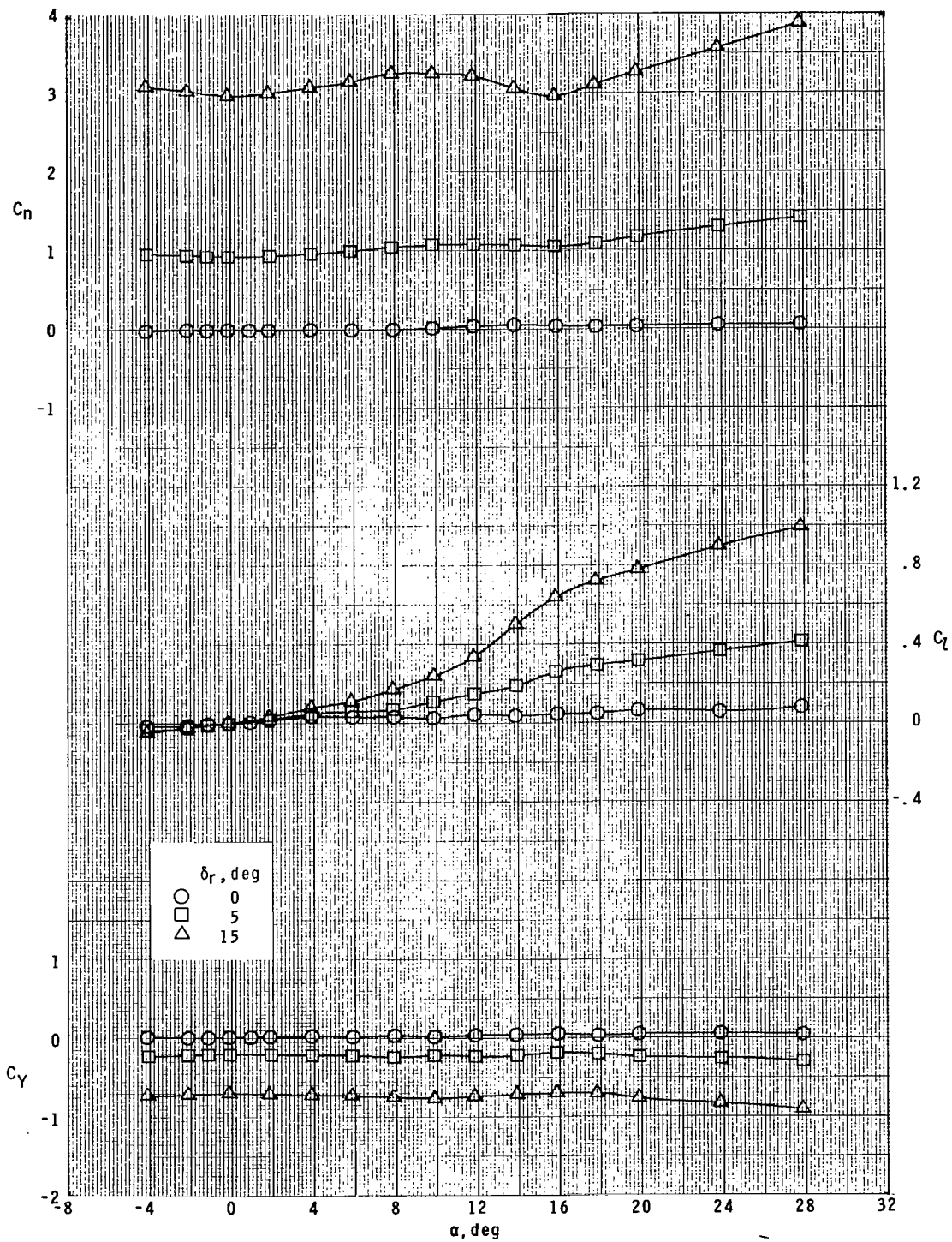
Figure 12.- Yaw control characteristics for body-tail<sub>1</sub>, cranked wing, nose strakes, and radar nose configuration.





(b)  $M = 2.16$ .

Figure 12.- Continued.



(c)  $M = 2.86$ .

Figure 12.- Concluded.

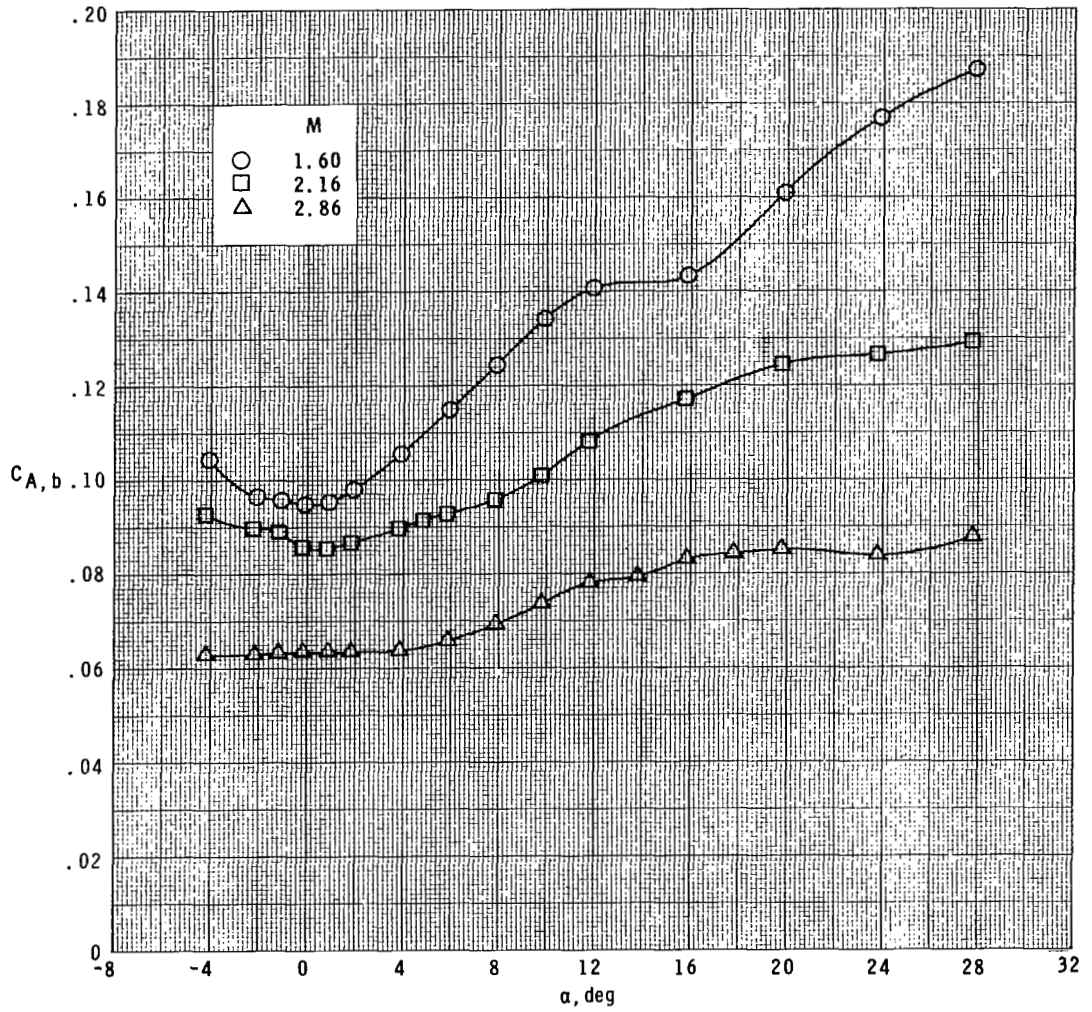


Figure 13.- Variation of base drag at angle of attack for body-tail<sub>1</sub>, cranked wing, nose strakes, and radar nose configuration.



1. Report No. NASA TP-1352		2. Government Accession No.		3. Recipient's Catalog No.	
4. Title and Subtitle STABILITY AND CONTROL CHARACTERISTICS OF A MONOPLANAR ELLIPTIC MISSILE MODEL AT MACH NUMBERS FROM 1.60 TO 2.86				5. Report Date February 1979	
				6. Performing Organization Code	
7. Author(s) Wallace C. Sawyer and Giuliana Sangiorgio				8. Performing Organization Report No. L-12268	
9. Performing Organization Name and Address NASA Langley Research Center Hampton, VA 23665				10. Work Unit No. 505-11-23-03	
				11. Contract or Grant No.	
12. Sponsoring Agency Name and Address National Aeronautics and Space Administration Washington, DC 20546				13. Type of Report and Period Covered Technical Paper	
				14. Sponsoring Agency Code	
15. Supplementary Notes					
16. Abstract  An investigation has been conducted of a monoplanar maneuverable missile concept having a nose forebody with a circular cross section and a centerbody and afterbody with elliptical cross sections. The tests involved several component changes and were conducted in the low Mach number test section of the Langley Unitary Plan wind tunnel at Mach numbers of 1.60, 2.16, and 2.86, at angles of attack ranging from $-4^{\circ}$ to $28^{\circ}$ , and at sideslip angles ranging from $-4^{\circ}$ to $8^{\circ}$ . The most significant result was that at the highest Mach number (2.86), the configuration with the infrared nose produced nearly twice the axial force as the same configuration with the radar nose. The cranked wing had a destabilizing effect on the longitudinal stability and had no effect on the lateral-directional stability. The nose strakes had no effect longitudinally and were detrimental to the lateral-directional stability.					
17. Key Words (Suggested by Author(s))  Monoplanar missile Missile stability control Missile aerodynamics			18. Distribution Statement  Unclassified - Unlimited  Subject Category 02		
19. Security Classif. (of this report) Unclassified	20. Security Classif. (of this page) Unclassified	21. No. of Pages 46	22. Price* \$4.50		

\* For sale by the National Technical Information Service, Springfield, Virginia 22161

NASA-Langley, 1979

National Aeronautics and  
Space Administration

THIRD-CLASS BULK RATE

Postage and Fees Paid  
National Aeronautics and  
Space Administration  
NASA-451



Washington, D.C.  
20546

Official Business  
Penalty for Private Use, \$300

5 1 1U, A, 020279 S00903DS  
DEPT OF THE AIR FORCE  
AF WEAPONS LABORATORY  
ATTN: TECHNICAL LIBRARY (SUL)  
KIRTLAND AFB NM 87117

**NASA**

**S**

POSTMASTER:

If Undeliverable (Section 158  
Postal Manual) Do Not Return